

NIST Technical Note TN 1685

Modeling Smoldering Fires using the Computer Model CONTAM

William D. Davis

NIST Technical Note TN 1865

Modeling Smoldering Fires using the Computer Model CONTAM

William D. Davis
*Engineering Laboratory
Fire Research Division
National Institute of Standards and Technology
Gaithersburg, MD 20899-8664*

December, 2010



U.S. Department of Commerce
Gary Locke, Secretary

National Institute of Standards and Technology
Patrick D. Gallagher, Director

Certain commercial entities, equipment, or materials may be identified in this document in order to describe an experimental procedure or concept adequately. Such identification is not intended to imply recommendation or endorsement by the National Institute of Standards and Technology, nor is it intended to imply that the entities, materials, or equipment are necessarily the best available for the purpose.

**National Institute of Standards and Technology Technical Note 1865
Natl. Inst. Stand. Technol. Tech. Note 1865, 51 pages (December, 2010)**

Contents

Table of Figures.....	vi
Abstract	1
Introduction.....	1
Experiments.....	2
Computer Model	3
CONTAM.....	3
Experiment JR-18.....	5
Modeling JR-18 using CONTAM.....	5
Experiment JR-17.....	12
Modeling JR-17 using CONTAM.....	13
Experiment JR-19.....	21
Modeling JR – 19 using CONTAM	22
Optical Density Comparison	30
Uncertainty.....	34
Conclusion.....	35
Appendix A	37
References	43

Table of Figures

Figure 1 JR-18, Bedroom A, NRC Peak Model and Constant Source (CS) Model	7
Figure 2 JR-18 Difference between measured (m) and predicted (p) percent visibility for bedroom A using the Constant Source (CS) and NRC Peak Models.....	8
Figure 3 JR-18, Hallways, Constant Source Model. “p” denotes predicted results.....	9
Figure 4 JR-18 Difference between measured (m) and predicted (p) percent visibility for hallways C and J, Constant Source. H stands for hallways.....	10
Figure 5 JR-18, Hallways, NRC Peak Model. “p” denotes predicted results.....	11
Figure 6 JR-18 Difference between measured (m) and predicted (p) percent visibility for hallways C and J, NRC Peak Model. H stands for hallways.....	12
Figure 7 JR-17 Bedroom comparisons, JR-17 Constant Source model. “p” denotes predicted results. ...	14
Figure 8 JR-17 Difference between measured (m) and predicted (p) percent visibility for bedrooms A, B, and F, Constant Source. Bd stands for bedroom.....	15
Figure 9 JR-17, Bedroom comparisons, NRC Peak model. “p” denotes model results.....	16
Figure 10 JR-17 Difference between measured (m) and predicted (p) percent visibility for bedrooms A, B, and F, NRC Peak Model. Bd stands for bedroom.....	17
Figure 11 JR-17, Hallway comparisons, Constant Source model. “p” denotes predicted results.....	18
Figure 12 JR-17 Difference between measured (m) and predicted (p) percent visibility for hallways C and J, Constant Source. H stands for hallways.....	19
Figure 13 JR-17, Hallway comparisons, NRC peak model. “p” denotes predicted results.....	20
Figure 14 JR-17 Difference between measured (m) and predicted (p) percent visibility for hallways C and J, NRC Peak Model. H stands for hallways.....	21
Figure 15 JR-19 Bedroom comparisons, Constant Source model. “p” denotes predicted results.....	23
Figure 16 JR-19 Difference between measured (m) and predicted (p) percent visibility for bedrooms A, B, and F, Constant Source. Bd stands for bedroom.....	24
Figure 17 JR-19 bedroom comparisons, NRC peak model. “p” denotes predicted results.....	25
Figure 18 JR-19 Difference between measured (m) and predicted (p) percent visibility for bedrooms A, B, and F, NRC Peak Model. Bd stands for bedroom.....	26
Figure 19 JR-19 hallway comparison, Constant Source. “p” denotes predicted results.....	27
Figure 20 JR-19 Difference between measured (m) and predicted (p) predicted visibility for hallways C and J, Constant Source. H stands for hallways.....	28
Figure 21 JR-19 hallway comparison, NRC peak model. “p” denotes predicted results.....	29
Figure 22 JR-19 Difference between measured (m) and predicted (p) percent visibility for hallways C and J, NRC Peak Model. H stands for hallways.....	30
Figure 23 Comparison of the measured optical density at the ceiling for the three experiments. Measurement points are shown at 300 s intervals.....	32
Figure 24 Optical densities for the three experiments measured 1.5 m (5 ft) above the floor. Measurement points are shown at 300 s intervals.....	33
Figure 25 Percent difference between the optical density at the ceiling (c) and at a height of 1.5 m (5 ft) above the floor (1.5) for the three experiments.....	34
Figure 26 first floor with all bedroom doors open.....	37

Figure 27 second floor with all bedroom doors open.....	38
Figure 28 basement with all bedroom doors open. The furnace is located in space Z.....	39
Figure 29 first floor with all bedroom doors closed.....	40
Figure 30 second floor with all bedroom doors closed.....	41
Figure 31 basement with all bedroom doors closed. The furnace is located in space Z.....	42

Abstract

The NIST computer model CONTAM was used to simulate the spread of smoke in a house with a working furnace during smoldering fires. Three smoldering experiments from a study on detector sensitivity and siting requirements conducted in 1975 using a two-story brick house with a basement were chosen to compare with the model. The choice was based on the experiments having similar smoldering sources and location, a furnace that was operated in two of the experiments, the reported doors to various rooms being open or closed and the outdoor weather having almost identical conditions. All of these experimental fires smoldered for a substantial length of time and did not transition to flaming. The results of the modeling are compared with the experiments. CONTAM was not designed to model fire effects, but with some recommended additions could become very useful modeling smoke spread from smoldering fires.

Key words: smoldering; fire experiments; computer modeling; HVAC; visibility

Introduction

Predicting the movement of smoke and toxic gases in a residential setting is complicated and depends on the type of fire (smoldering or flaming), the impact of the heating, ventilation and air conditioning system (HVAC), the status of windows and doors, and the weather outside the residence. A smoldering fire is a slow, low-temperature, flameless form of combustion¹ where the HVAC system in the residence may play a significant role in the movement of smoke and toxic gases. A flaming fire is a high-temperature phenomenon where the movement of smoke and toxic gases is typically buoyancy-driven by the fire. Examining the capabilities of a computer model to simulate the spread of smoke in a house with a working furnace during a smoldering fire is the objective of this paper.

Three smoldering experiments from a study on detector sensitivity and siting requirements conducted in 1975 using a two-story brick house with a basement were chosen to model. This choice was based on the experiments having similar smoldering sources and location, a furnace that was operated in two of the experiments, the reported doors to various rooms being open or closed and the outdoor weather having almost identical conditions². All of these experiments smoldered for a substantial length of time and did not transition to flaming.

The computer model analyzed in this paper is CONTAM³. CONTAM is a one-zone simulation model and provides several methods to model HVAC systems. It does not use a buoyancy-driven plume model to represent the source of the smoke. Details of each experiment and how the model was applied are discussed in the next sections.

Abstract

The NIST computer model CONTAM was used to simulate the spread of smoke in a house with a working furnace during smoldering fires. Three smoldering experiments from a study on detector sensitivity and siting requirements conducted in 1975 using a two-story brick house with a basement were chosen to compare with the model. The choice was based on the experiments having similar smoldering sources and location, a furnace that was operated in two of the experiments, the reported doors to various rooms being open or closed and the outdoor weather having almost identical conditions. All of these experimental fires smoldered for a substantial length of time and did not transition to flaming. The results of the modeling are compared with the experiments. CONTAM was not designed to model fire effects, but with some recommended additions could become very useful modeling smoke spread from smoldering fires.

Key words: smoldering; fire experiments; computer modeling; HVAC; visibility

Introduction

Predicting the movement of smoke and toxic gases in a residential setting is complicated and depends on the type of fire (smoldering or flaming), the impact of the heating, ventilation and air conditioning system (HVAC), the status of windows and doors, and the weather outside the residence. A smoldering fire is a slow, low-temperature, flameless form of combustion¹ where the HVAC system in the residence may play a significant role in the movement of smoke and toxic gases. A flaming fire is a high-temperature phenomenon where the movement of smoke and toxic gases is typically buoyancy-driven by the fire. Examining the capabilities of a computer model to simulate the spread of smoke in a house with a working furnace during a smoldering fire is the objective of this paper.

Three smoldering experiments from a study on detector sensitivity and siting requirements conducted in 1975 using a two-story brick house with a basement were chosen to model. This choice was based on the experiments having similar smoldering sources and location, a furnace that was operated in two of the experiments, the reported doors to various rooms being open or closed and the outdoor weather having almost identical conditions². All of these experiments smoldered for a substantial length of time and did not transition to flaming.

The computer model analyzed in this paper is CONTAM³. CONTAM is a one-zone simulation model and provides several methods to model HVAC systems. It does not use a buoyancy-driven plume model to represent the source of the smoke. Details of each experiment and how the model was applied are discussed in the next sections.

Experiments

Flaming and smoldering experiments were conducted in a two-story brick house with a full basement². A plan view of the house is provided in appendix A. The interior walls on the first and second stories were plaster on wood lath and the floors were wood. The walls in the basement were wood paneled.

A forced air furnace used for heating was located in the basement with outlet registers located in every room of the house. Return air grilles were located on the first floor but there were no returns on the second floor. All the bedroom doors had undercuts which allowed for a return air flow from the second floor bedrooms³. The geometry of the undercuts was not provided in the report. Floor plans showing register and return locations and flow rates are provided in Appendix A.

Instrumentation for the experiments included white-light beams for measuring smoke obscuration at the ceiling in the fire room, at the ceiling for each detector location, and at the 1.5 m (5 ft) level along the primary escape path and in representative bedrooms. The light beams had 1.5 m (5 ft) beam lengths. Individual thermocouples and vertical thermocouple arrays were installed in the fire room, the primary escape path and several representative locations throughout the dwelling. The Heat Release Rate (HRR) and mass-loss rate of the smoldering materials were not measured during the experiments.

Three smoldering experiments from the winter bedroom series (JR-17, JR-18, and JR-19) were modeled. The smoldering fire for each of these tests was located in the first floor bedroom A. Furnace and door conditions are given in Table 1. The doors and windows to the outside were closed. The fuel source for each experiment was a smoldering cotton mattress.

Experiment	Furnace	Bedroom Door A (Fire Room)	Other Bedroom Doors
JR-17	Operating	Open	Open
JR-18	Not Operating	Open	Closed
JR-19	Operating	Closed	Closed

Table 1 Door and Furnace conditions for each experiment

Flaming was not observed during any of the tests. A 500 W charcoal igniter with approximately 0.5 m (20 in) of exposed cal-rod and energized from 120 V ac was used to ignite the cotton mattresses.

Weather conditions may impact the flow of smoke, particularly if there is significant wind and a leaky building envelope. For these experiments, weather conditions were almost identical as shown in Table 2.

Experiment	Outdoor Temperature °C (°F)	Outdoor Relative Humidity (%)	Wind Direction	Nominal Wind Speed km/h (mph)	Peak Wind Gust km/h (mph)
JR - 17	0 (32)	84	W	2.6 – 4.4 (1.6 – 2.7)	9.5 (5.9)
JR - 18	1 (34)	90	W – SW	2.2 – 3.3 (1.4 – 2.0)	6.0 (3.7)
JR – 19	1 (34)	72	W - SW	1.1 – 3.3 (0.7 – 3.3)	10. (6.2)

Table 2 Weather conditions

The timing of the wind gusts and the orientation of the house were not provided in the report.

Computer Model

The computer model used for this comparison, CONTAM⁴, has the capability to simulate the air flow produced by a furnace. In the following paragraphs, CONTAM will be briefly described and the approximations used to model the experiments examined.

CONTAM

CONTAM is a multizone indoor air quality and ventilation analysis computer program designed to help determine:

- *Airflows*: infiltration, exfiltration, and room-to-room airflows in building systems driven by mechanical means, wind pressures acting on the exterior of the building, and buoyancy effects induced by the indoor and outdoor air temperature difference.
- *Contaminant Concentrations*: the dispersal of airborne contaminants transported by these airflows; transformed by a variety of processes including chemical and radio-chemical transformation, adsorption and desorption to building materials, filtration, and deposition to building surfaces, etc.; and generated by a variety of source mechanisms.

For this application, the contaminant was the smoke produced by a smoldering mattress. It should be noted that CONTAM was not designed to handle fire situations and is lacking certain features that are needed to make the model predictive under these circumstances. The use of the model here was to explore its use for predicting smoke spread in smoldering fire situations where the application of fire models based on buoyant plumes would be inappropriate. The model was initiated by representing each room in the house as a zone with a temperature, pressure, and smoke concentration. The ventilation system air flows were represented using the simple air-handling system (AHS). This AHS provides a convenient means of incorporating an air-handling system into a building without having to draw and define an entire duct system. Each simple air-handling system consists of two implicit airflow nodes or zones (*supply* and *return* sub-systems), three implicit flow paths (*recirculation*, *outdoor*, and *exhaust*), and

multiple *zone supplies* (inlets to zones) and *zone returns* (outlets from zones) that can be placed within zones throughout the building. The airflow rates of each *supply* and *return* point are specified. Simple air-handling systems do not require an association of both zone supplies and zone returns with them. The simple air-handling system may be set to only supply outdoor (ambient) air to a building or to only exhaust air from the building. The AHS was set to recirculate the air in the house and not introduce outside air for this analysis. The amount of outside air introduced by the furnace was not provided in the report⁴.

Thermal effects – The model does not handle heat transfer phenomena per se, but does provide for the scheduling of zone temperatures. Zone temperatures can be either constant or allowed to change during transient simulations according to user-defined temperature schedules. CONTAM will determine airflows and non-trace contaminant mass fractions induced by temperature differences between zones including ambient (e.g., as caused by the stack effect). This feature was used when sufficient temperature data was available to use a temperature schedule. A linear variation in time was used to change the temperature in a zone from its initial value to a final value when only the initial and final temperatures were available.

The smoldering fires for these experiments were approximated using two different models. The first model was the constant source model⁴

$$S(t) = G + D * C(t)$$

where $S(t)$ is the smoke source in the zone in $\mu\text{g/s}$, G is the generation rate of smoke in $\mu\text{g/s}$. D was set to zero as this term represents the removal rate of the smoke, and it was assumed that smoke deposition to the walls was negligible. The value of G was varied until the smoke density in the fire room was consistent with the measured light extinction in the fire room at the end of the experiment. For a smoldering fire, the decrease in light intensity due to the smoke is calculated using the extinction coefficient per unit mass $k_m = 4.4 \text{ m}^2/\text{g}$,⁵ and is given by $I = I_0 e^{-4.4\rho x}$ where ρ is the smoke density in g/m^3 , x is the length of the light path in meters, I is the measured light intensity at length x and I_0 is the initial light intensity.⁶ The light path used in the experiments was equal to 1.5 m (5 ft). Since CONTAM expresses smoke densities as ratios to the density of air ($1,204 \text{ g/m}^3$ at 20°C and 1 atm.), the final form of the equation that was used to determine the visibility as a function of smoke density ρ was

$$\text{visibility} = \frac{I}{I_0} = e^{-\left[\left(\frac{\rho}{\rho_{air}}\right) * 4.4 * 1204 * 1.5\right]}$$

The second model used to represent the smoldering fires was the NRC Peak Model⁴. This model permits the amount of smoke emitted during smoldering to increase with time using the relationship

$$S(t) = ae^{-.5\left[\frac{\ln\left(\frac{t}{t_p}\right)}{b}\right]^2}$$

where a is the value of $S(t)$ ($\mu\text{g/s}$) at time t_p and b is a dimensionless fitting parameter. The constants for this model were evaluated by matching the measured visibility in the fire room at the end of the experiment and at the halfway point to the visibility that would be deduced using the smoke density predicted by CONTAM and the relationship for the decrease in light intensity due to smoldering smoke.

The two-way flow model⁴ was used to model open doors while the power law crack model⁴ was used to represent closed doors. The closed bedroom doors presented an uncertainty as the doors had undercuts of an unknown size. The undercuts were modeled with dimensions equal to the door width, 2.4 m and a height of 0.025 m (0.10 in). The power law exponent was 0.5.⁴ There were also two doors that opened to the outdoors. The power law crack model was used to model these doors with the crack equal to the width of the door with a height of 0.00025 m (.0010 in) and a power law exponent of 0.94.⁴

Experiment JR-18

This smoldering experiment was conducted with the furnace turned off and all the bedroom doors except the one to the fire room (bedroom A) closed. The flow of smoke through parts of the house that were open should be dominated by the small temperature differences between hallways and rooms due to the heat from the smoldering cotton mattress and the loss of heat through the doors, windows and walls as the outside temperature was close to freezing, 1 °C – 2 °C (34 °F – 35 °F). The temperature changes in rooms throughout the house were recorded only as an initial temperature and a final temperature and these are listed in Table 1. The times that the final temperatures were reached were not given in the report.²

Room	Bed A	Bed B	Hallway C	Bed E	Bed F	Hallway J
Initial °C (°F)	21.7 (71)	23.3 (74)	18.0 (64.5)	18.3 (65)	20.0 (68)	21.7 (71)
Maximum °C (°F)	30.6 (87)	18.9 (66)	21.1 (70)	15.6 (60)	16.7 (62)	20.6 (69)

Table 3 Initial and final temperatures for JR-18

The cooling of the three bedrooms and the second floor Hallway J due to the furnace being off is evident from the table. The smoldering fire in bedroom A increased the temperature in Bedroom A and also heated the adjacent first floor Hallway C.

Modeling JR-18 using CONTAM

The temperatures were input into CONTAM as day schedules⁴ with the initial temperature used for the start of the experiment and the final temperature used for the end. A straight line fit connected the two temperatures and permitted extrapolation to other times. Rooms that did not have a temperature recorded were assumed to have the same initial temperature as an adjacent room and that temperature was treated as a constant during the calculation.

The smoldering fire was modeled as a smoke source using the Constant Source model and the NRC Peak model. A value of 19,000 $\mu\text{g/s}$ was used for the smoke input for the Constant Source model to match the measured visibility at the ceiling in bedroom A at 3,600 s. The constants used for the NRC Peak model include an initial smoke generation rate of 29,000 $\mu\text{g/s}$, 0.7 for the fitting constant, and 1.0 hr. for the peak time. These constants were chosen in order to approximate the measured visibility at the ceiling in bedroom A at 1,800 s and 3,600 s.

Both sources matched the measured visibility at the end of the experiment as shown in Figures 1 and 2. The Constant Source model underpredicts the visibility for most of the experiment while the NRC Peak Model source overpredicts the visibility for the first 1,000 s by less than 20 % and then the predictions are quite close (less than 10 % difference) to the measured visibility for the next 2,600 s. The lack of agreement using the Constant Source model is caused by the model assumption that the smoke output is a constant when it actually increased with time. Using the smoke output at the end of the experiment for the entire modeling period will yield too high of smoke output early in the experiment.

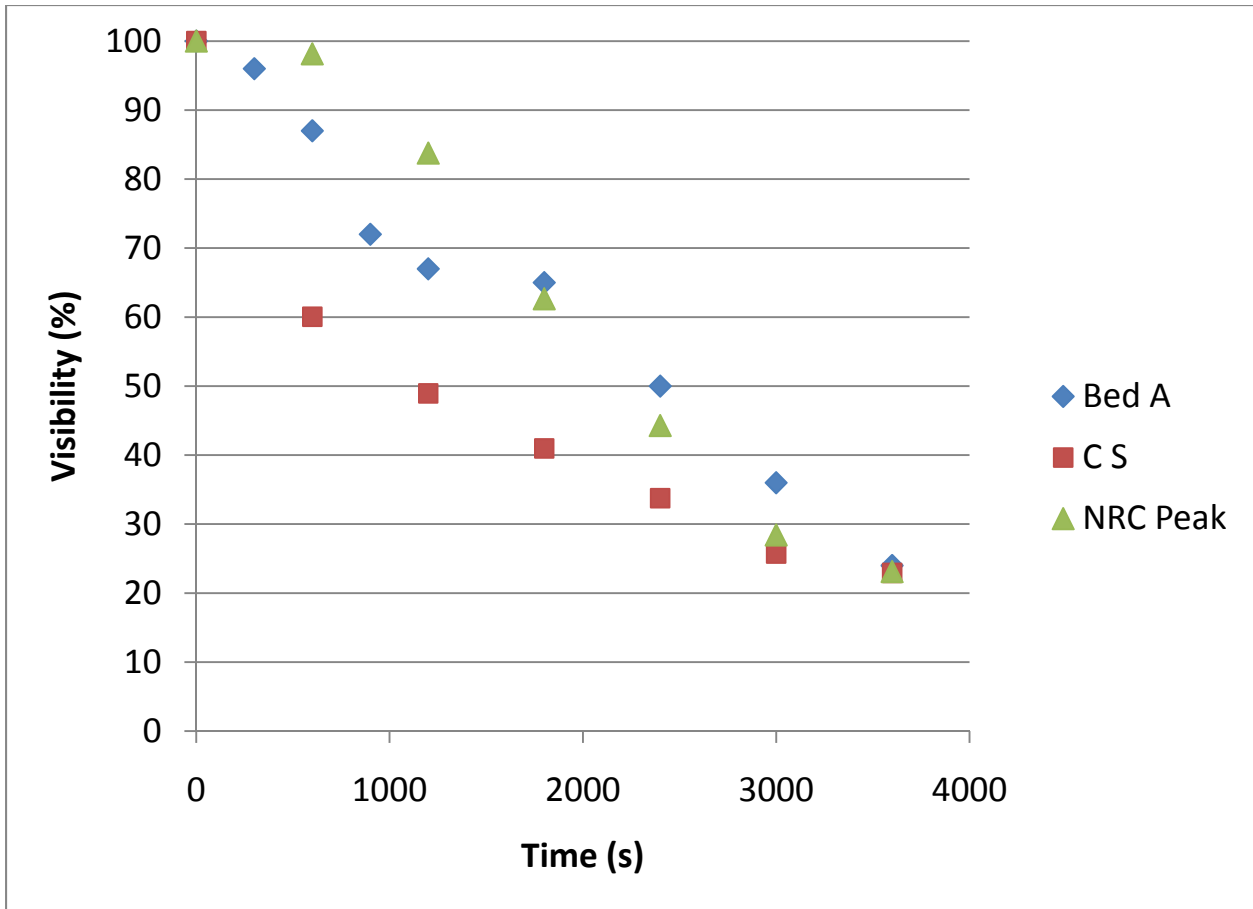


Figure 1 JR-18, Measurements in Bedroom A, NRC Peak Model and Constant Source (CS) Model

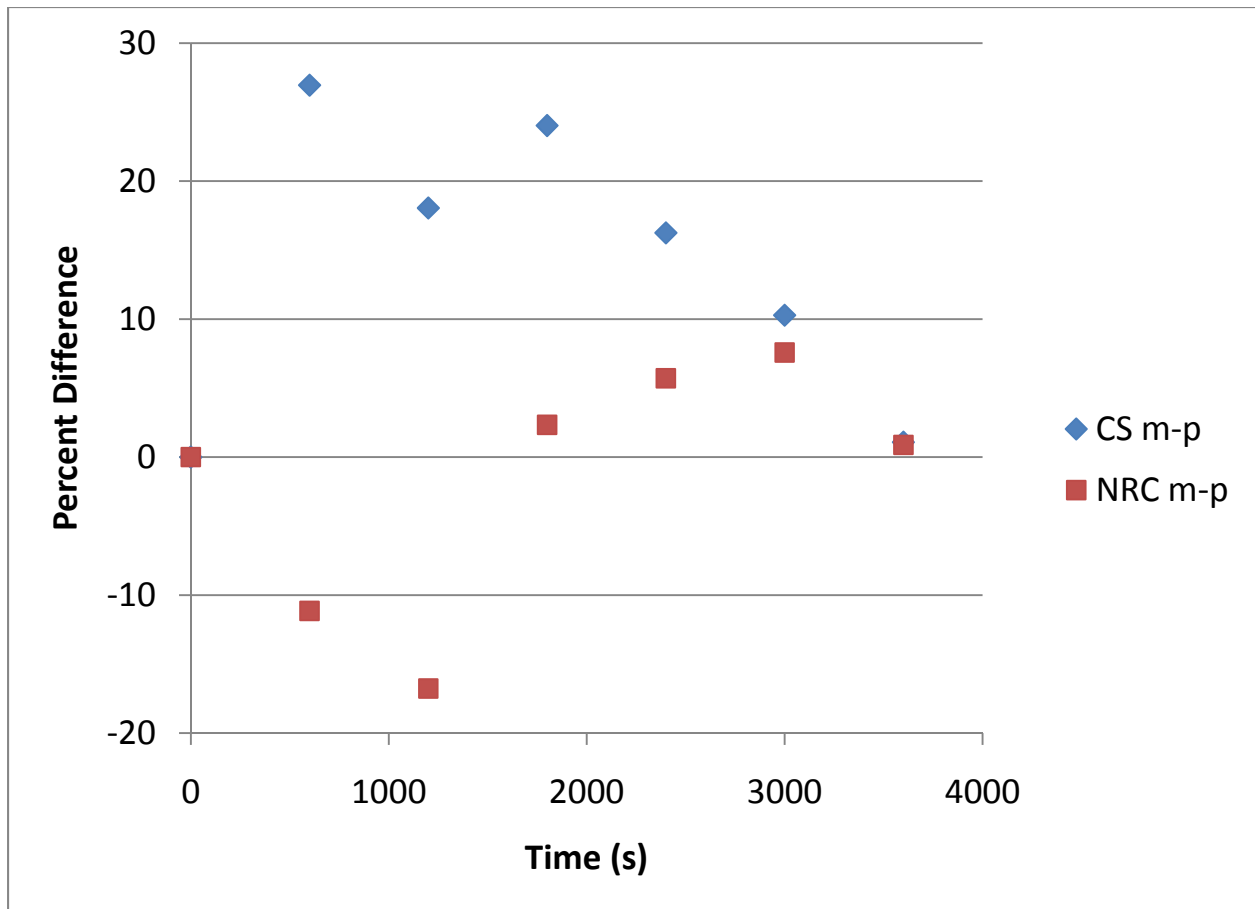


Figure 2 JR-18 Difference between measured (m) and predicted (p) percent visibility for bedroom A using the Constant Source (CS) and NRC Peak Models.

With the furnace off and the bedroom doors closed, the smoke spread to the other bedrooms was negligible as shown by the visibility measurement at the ceiling in Bedroom B which was still at 96% after 3600 s. Only the upstairs and downstairs hallways collected significant smoke and the smoke motion should be a result of diffusion and the changes in temperature. The hallway comparisons shown in Figure 2, Figure 3, Figure 4, and Figure 5 show that the Constant Source Model underpredicts the visibility through much of the experiment with differences generally greater than 20 % while the NRC Peak Model can be tuned to provide closer agreement to the visibility measurements with differences generally less than 20 %. The constant source model uses the same smoke output early in the fire as it does later in the fire and that causes the model to predict far less visibility than is actually experienced in the experiment.

The NRC Peak Model provided much better predictions of visibility in the hallways for the entire experiment than the constant source model. With the furnace being off, the upstairs hallway cooled and the visibility of the second floor hallway J became less than the first floor hallway C.

The CONTAM calculation using the NRC Peak Model predicts that the visibility of the second floor hallway J is less than the first floor hallway C although the predicted visibility difference is not as large as the measured value.

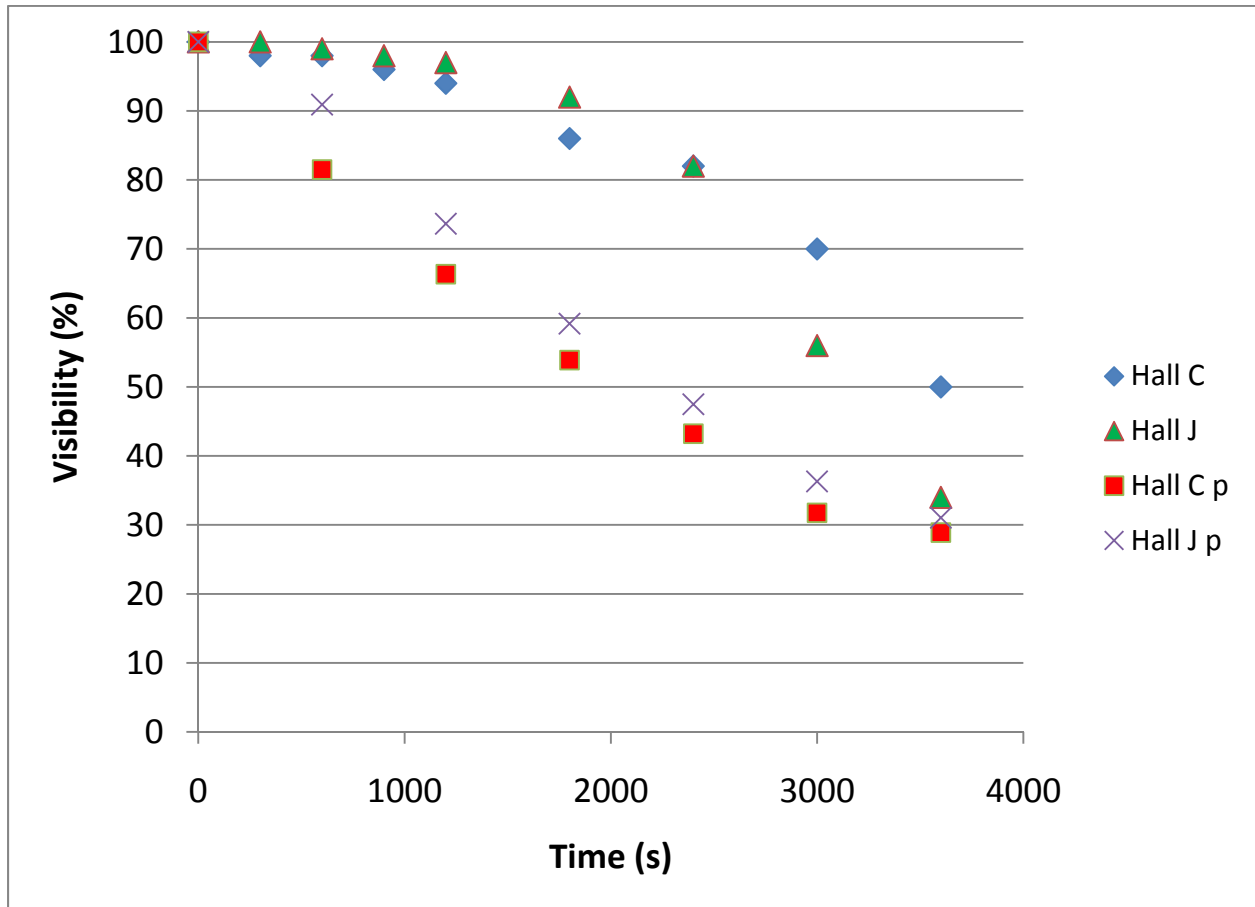


Figure 3 JR-18, Hallways, Constant Source Model. "p" denotes predicted results.

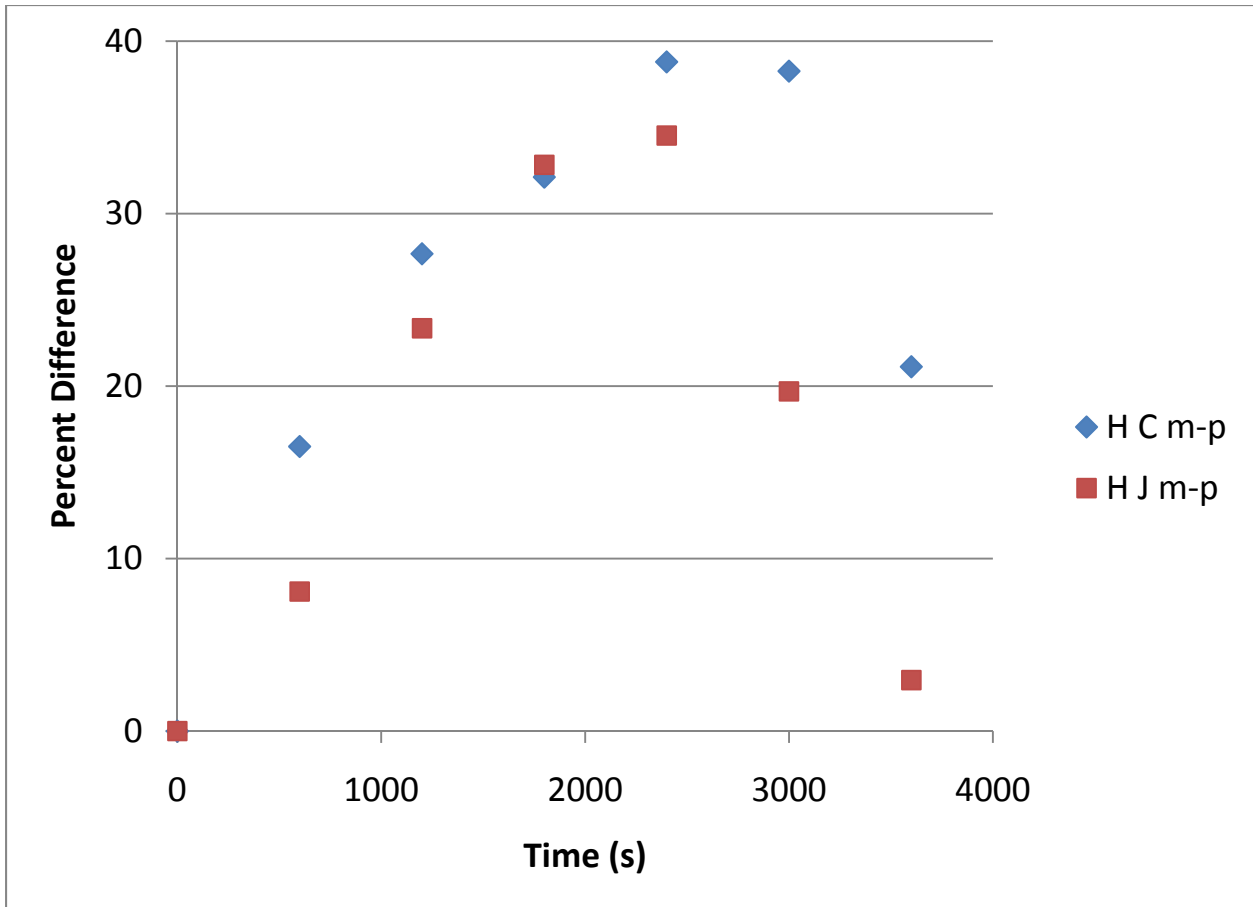


Figure 4 JR-18 Difference between measured (m) and predicted (p) percent visibility for hallways C and J, Constant Source. H stands for hallways.

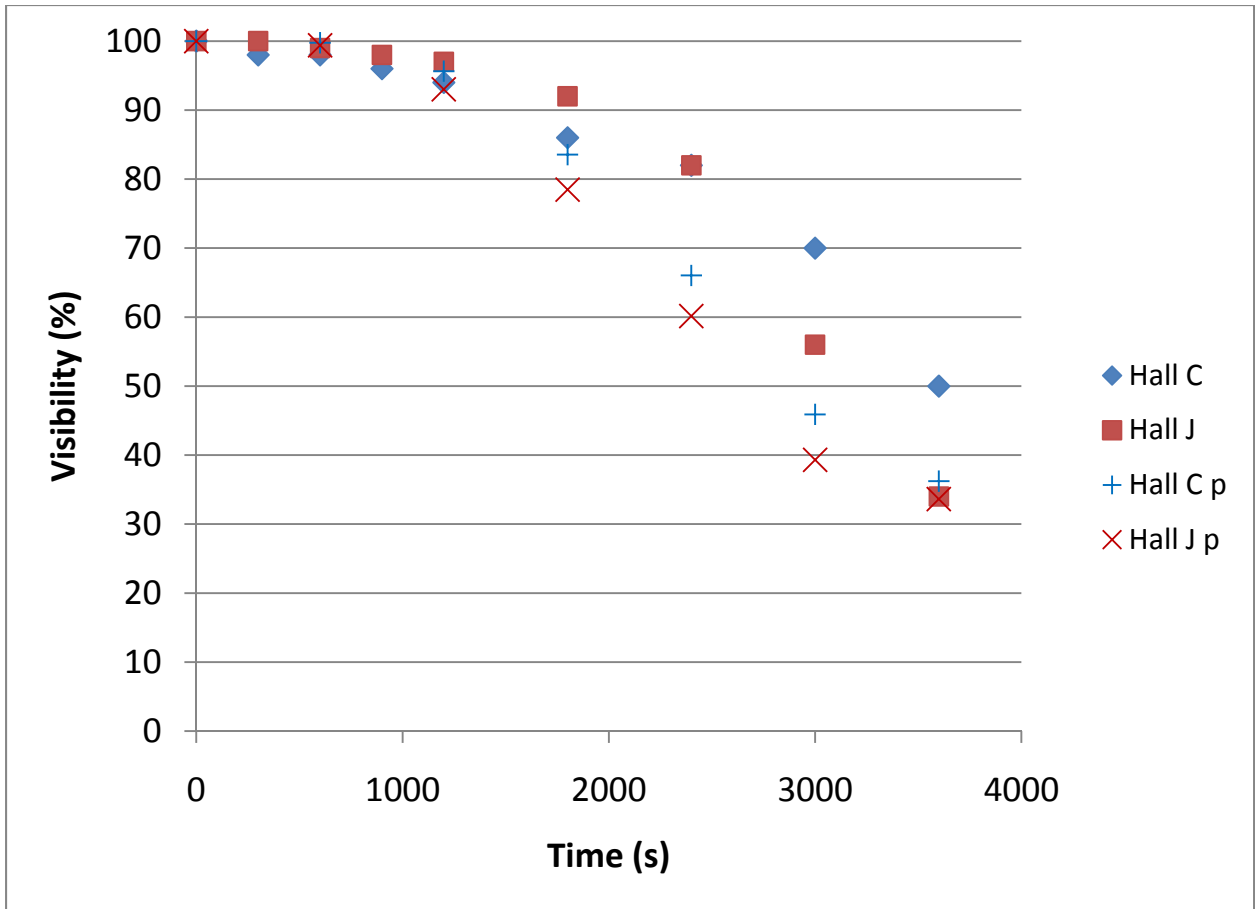


Figure 5 JR-18, Hallways, NRC Peak Model. "p" denotes predicted results.

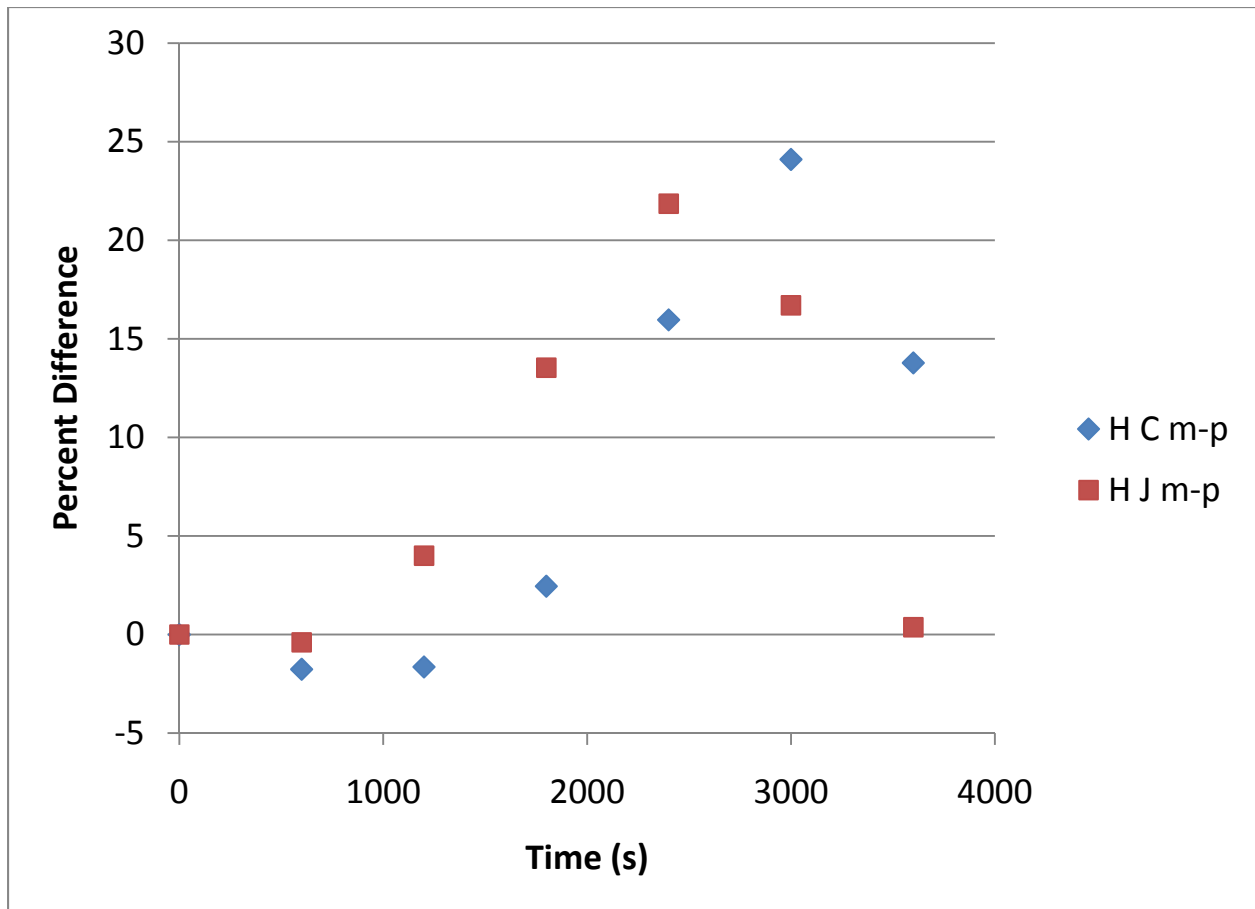


Figure 6 JR-18 Difference between measured (m) and predicted (p) percent visibility for hallways C and J, NRC Peak Model. H stands for hallways.

Experiment JR-17

This smoldering experiment was conducted with the furnace turned on and all the bedroom doors open. The flow of smoke through the house should result from the air flow produced by the furnace and by the small temperature differences that are caused by the production of heat from the smoldering cotton mattress, the heating of the furnace and the loss of heat through the doors, windows and walls as the outside temperature was at freezing, 0 °C (32 °F) during the experiment. The temperature changes in rooms throughout the house were recorded only as an initial temperature and a final temperature and these are listed in table 4. A temperature/time history was provided for bedroom A with the temperature only reaching 23.9 °C (75 °F) rather than the 32.2 °C (90 °F) as shown in table 4. For the modeling, the measured temperature history for bedroom A was used in the day schedule for that room but the initial temperatures shown in table 4 were used for the other bedrooms and the hallways. Table 5 displays bedroom A temperatures in time during the experiment.

Room	Bed A	Bed B	Hallway C	Bed E	Bed F	Hallway J
Initial (°C)	20.3	20.6	21.7	17.8	18.3	18.9
(°F)	68.5	69	71	64	65	66
final (°C)	32.2	23.3	22.8	18.3	18.6	20
(°F)	90	74	73	65	65.5	68

Table 4 Initial and final temperatures for JR-17

Time (s)	0	300	600	1,500	2,100	2,700	3,000	3,600
Temperature (°C)	20.3	22.8	22.2	22.8	23.3	22.8	23.3	23.9
(°F)	68.5	73	72	73	74	73	74	75

Table 5 Bedroom A temperatures for JR-17

Rooms that did not have a temperature recorded were assumed to have the same initial temperature as an adjacent room and that temperature was treated as a constant during the calculation.

A thermocouple was attached to an inlet register in the living room to provide a measurement of the temperature flow to that room from the furnace. The temperature at the inlet register varied between 24.4 °C (76 °F) and 45 °C (113 °F) with the heating cycle turning on three times during the experiment. Flow velocities were provided for the inlet registers and returns but the time dependence was not given.

The furnace was operated on automatic and so the furnace blower should turn on at the start of the heating cycle and turn off near the end of the heating cycle. If the temperature rise measured by the thermocouple at the inlet register is used to determine the times for blower operation, the blower operated in the periods 0 s to 360 s, 1,500 s to 2,100 s, and 3,300 s to 3,900 s. Using this measurement for the blower operation, the furnace blower operated about 40% of the time. It was assumed for the modeling that the furnace blower operated only during these time periods and the measured flow rates for the outlet registers and returns were constant during this period. The flow rates for other time periods were taken to be zero.

Modeling JR-17 using CONTAM

The two-way flow model⁴ was used to model the air flow through the open doors. The smoldering fire was modeled as a smoke source using the Constant Source model⁴ and the NRC Peak model⁴. A value of 9,000 µg/s was used for the smoke input for the Constant Source model to match the measured visibility in bedroom A at 3600 s. The constants used for the NRC Peak model included a smoke input of 15,000 µg/s, 0.85 for the filtering constant, and 1.5 hr. for the peak time. These constants were chosen in order to approximate the measured visibility in bedroom A at 1800 s and 3600 s.

The Constant Source model, Figure 7 and Figure 8, approximated the measured visibility in bedroom A at the end of the experiment; it underestimated the visibility in the bedroom for all earlier times. The predictions of this model for bedroom B was also an underestimate of the visibility but the visibility predictions for bedroom F were close to the measured values. The NRC Peak model, Figure 9 and Figure 10, was able to match the measured visibility of bedroom A for all but the earliest times. It overestimated the visibility in bedroom F by, at most, 15 % and underestimated the visibility but provided a better estimate than the Constant Source model for bedroom B.

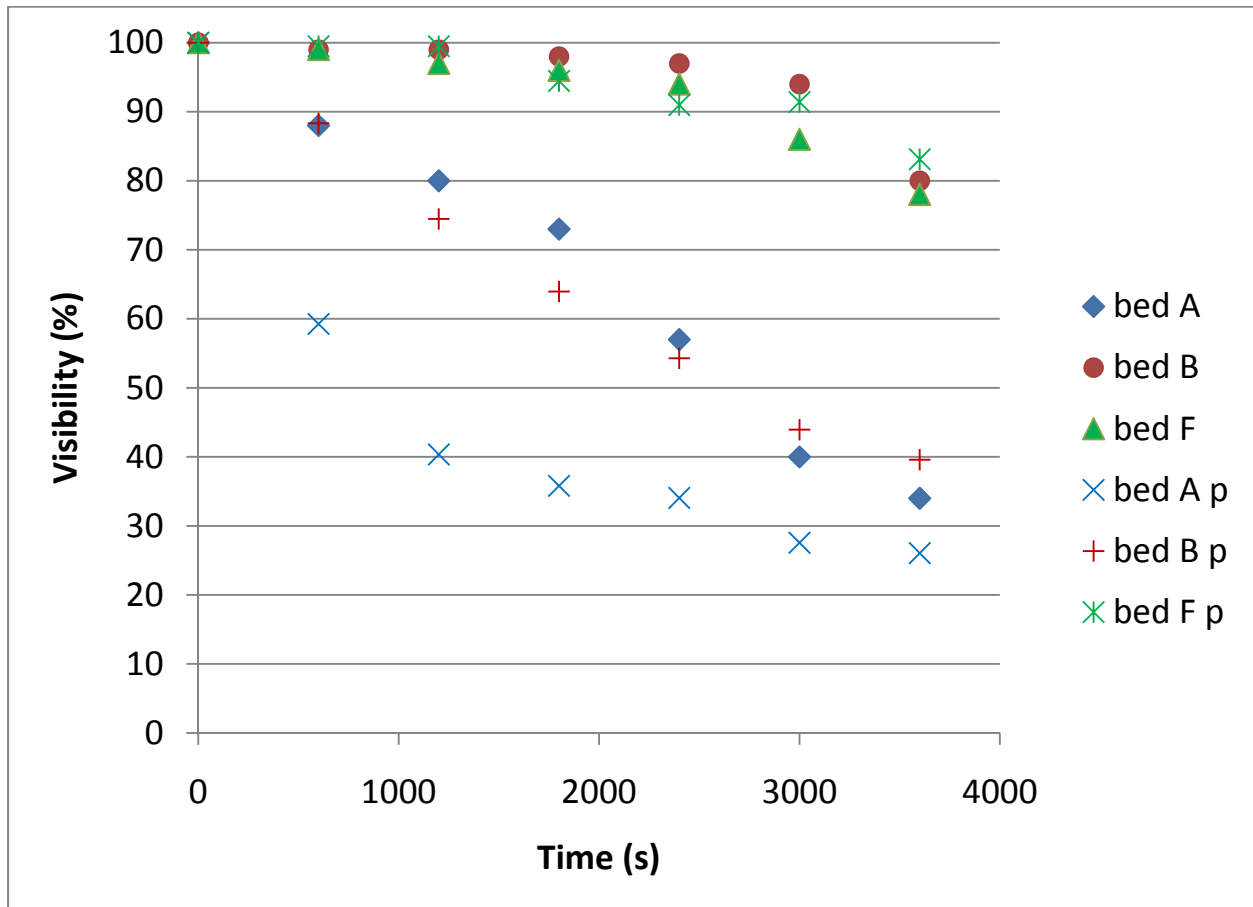


Figure 7 JR-17 Bedroom comparisons, JR-17 Constant Source model. “p” denotes predicted results.

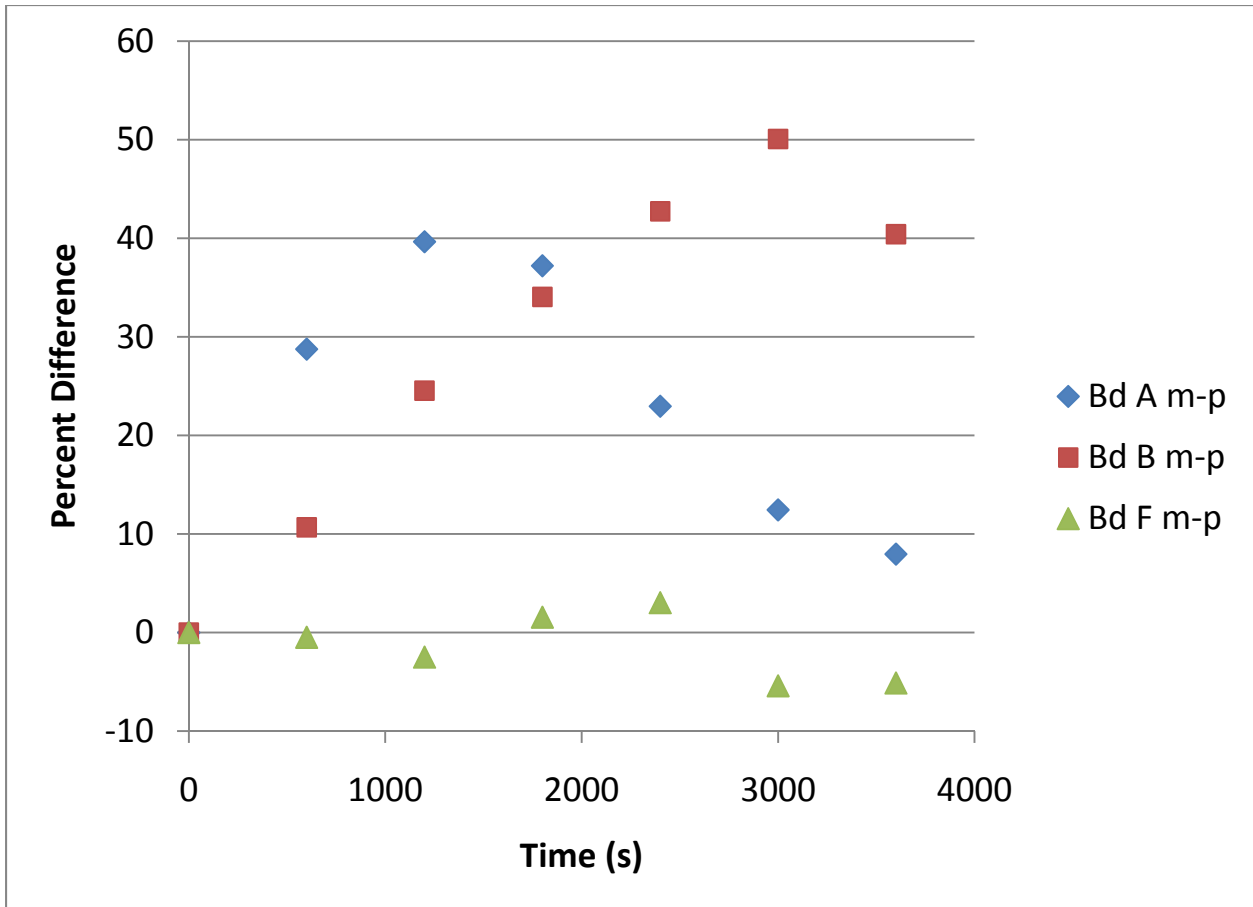


Figure 8 JR-17 Difference between measured (m) and predicted (p) percent visibility for bedrooms A, B, and F, Constant Source. Bd stands for bedroom.

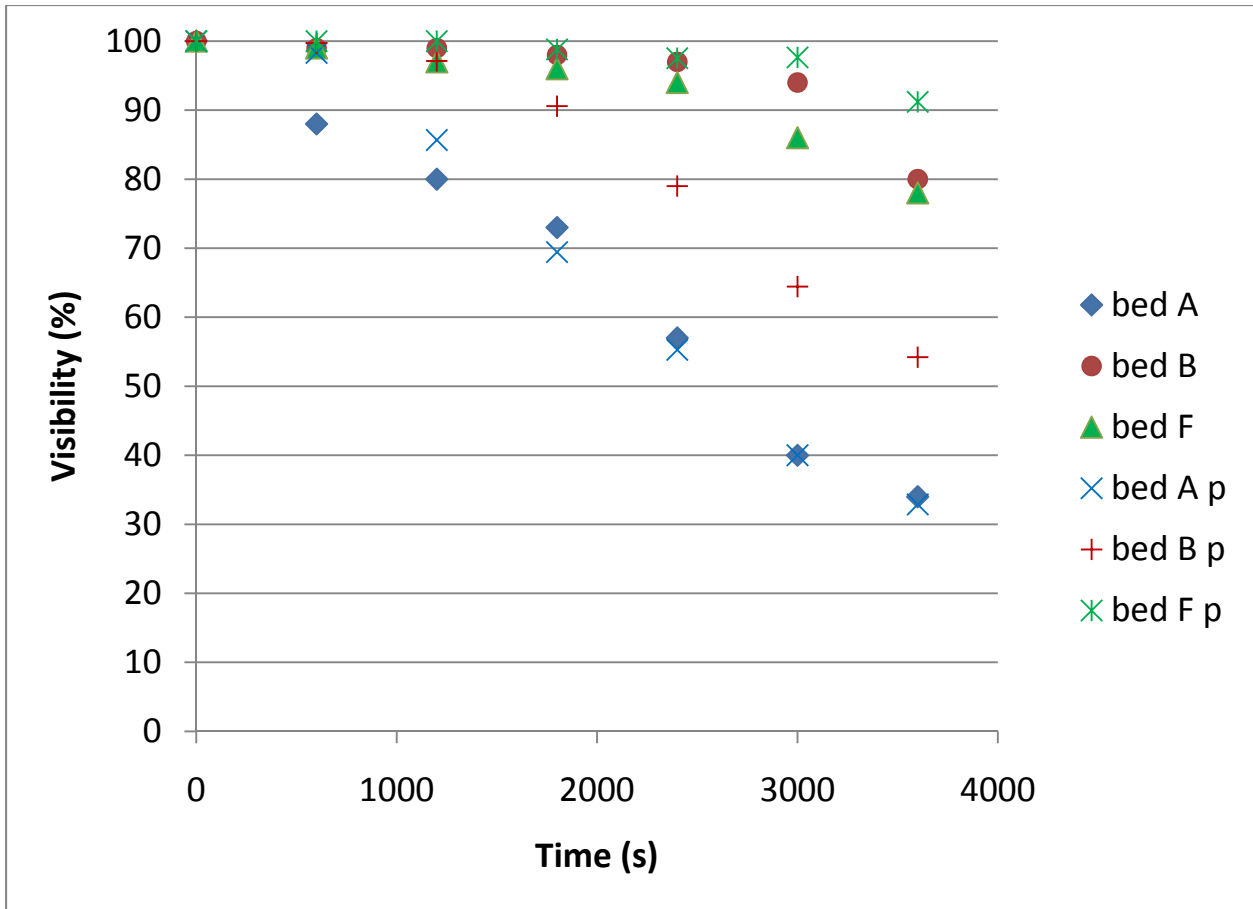


Figure 9 JR-17, Bedroom comparisons, NRC Peak model. "p" denotes model results.

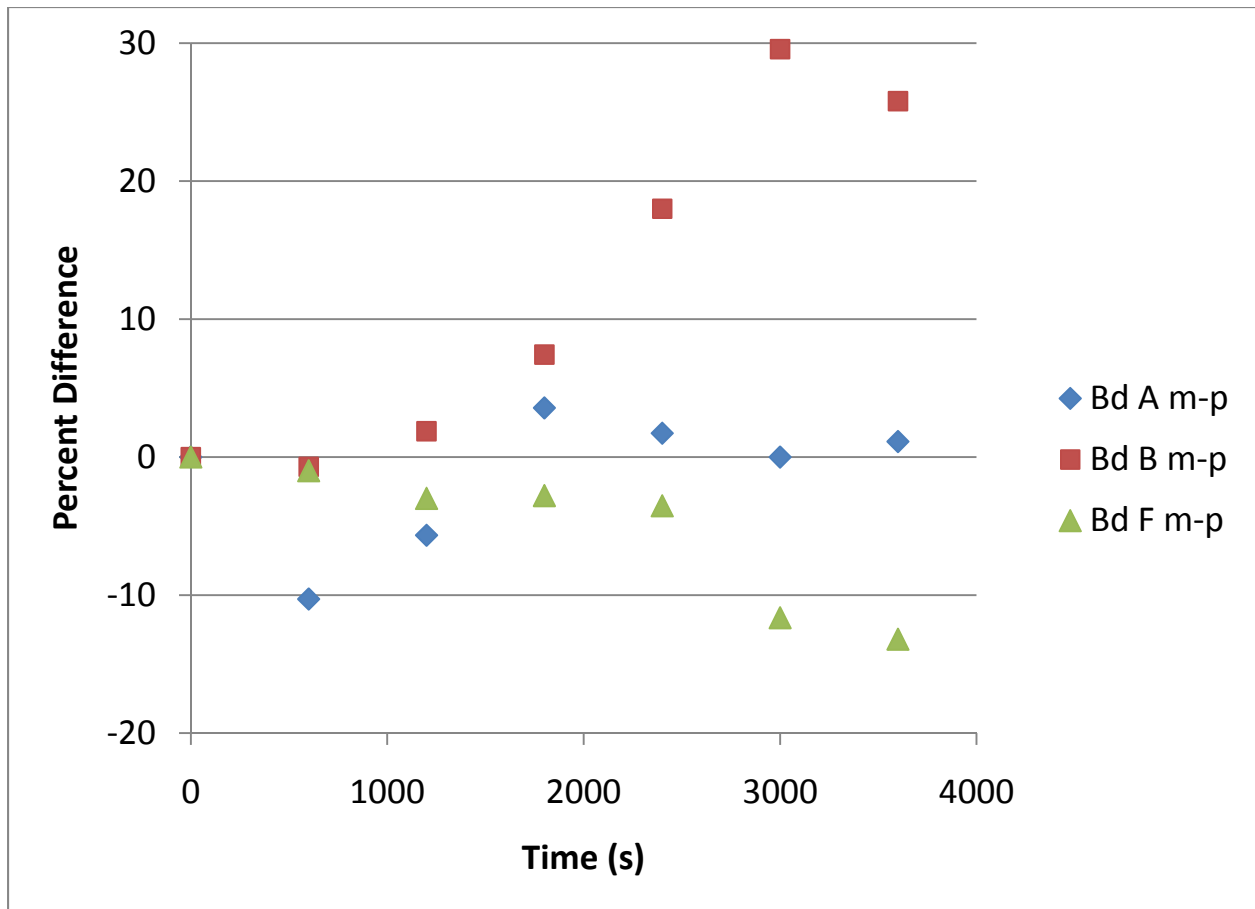


Figure 10 JR-17 Difference between measured (m) and predicted (p) percent visibility for bedrooms A, B, and F, NRC Peak Model. Bd stands for bedroom.

The comparison of the visibility in the two hallways (see Figure 11, Figure 12, Figure 13, and Figure 14) show close agreement (within $\pm 10\%$) between the measured visibility and the predicted visibility using the NRC Peak model. The constant source model predicts the visibility in the upstairs hallway J (within $\pm 5\%$) but underpredicts the visibility in the downstairs hallway C by 15% to 30%.

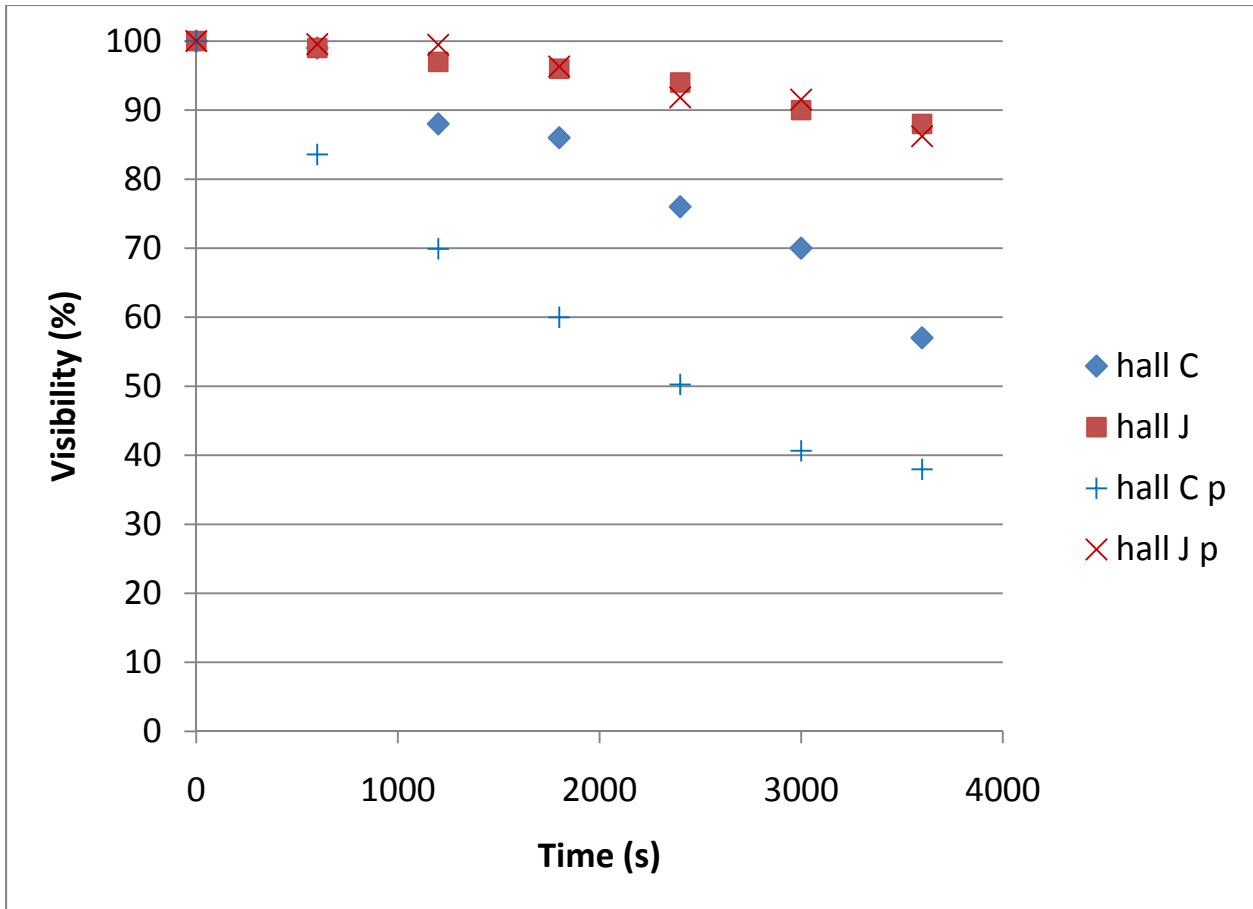


Figure 11 JR-17, Hallway comparisons, Constant Source model. “p” denotes predicted results.

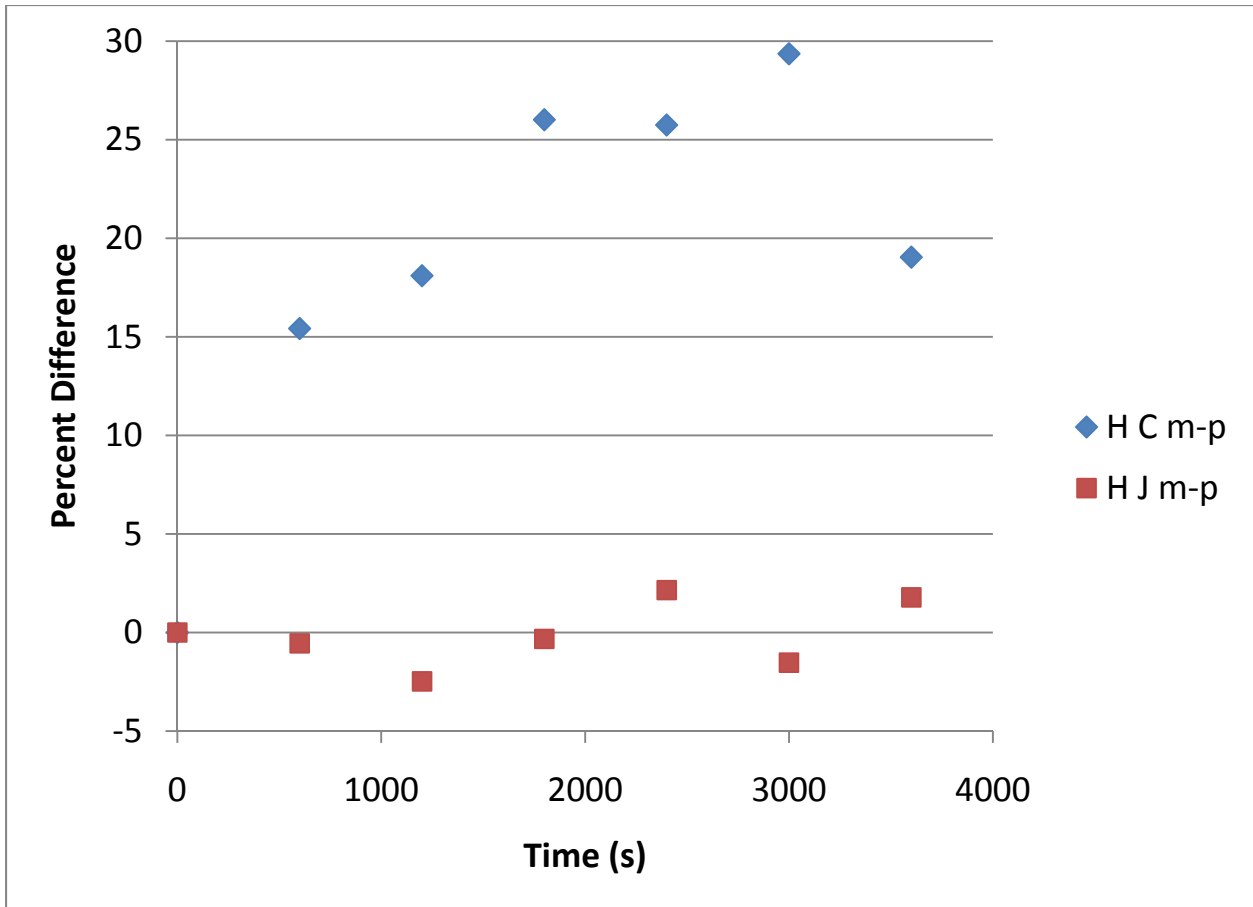


Figure 12 JR-17 Difference between measured (m) and predicted (p) percent visibility for hallways C and J, Constant Source. H stands for hallways.

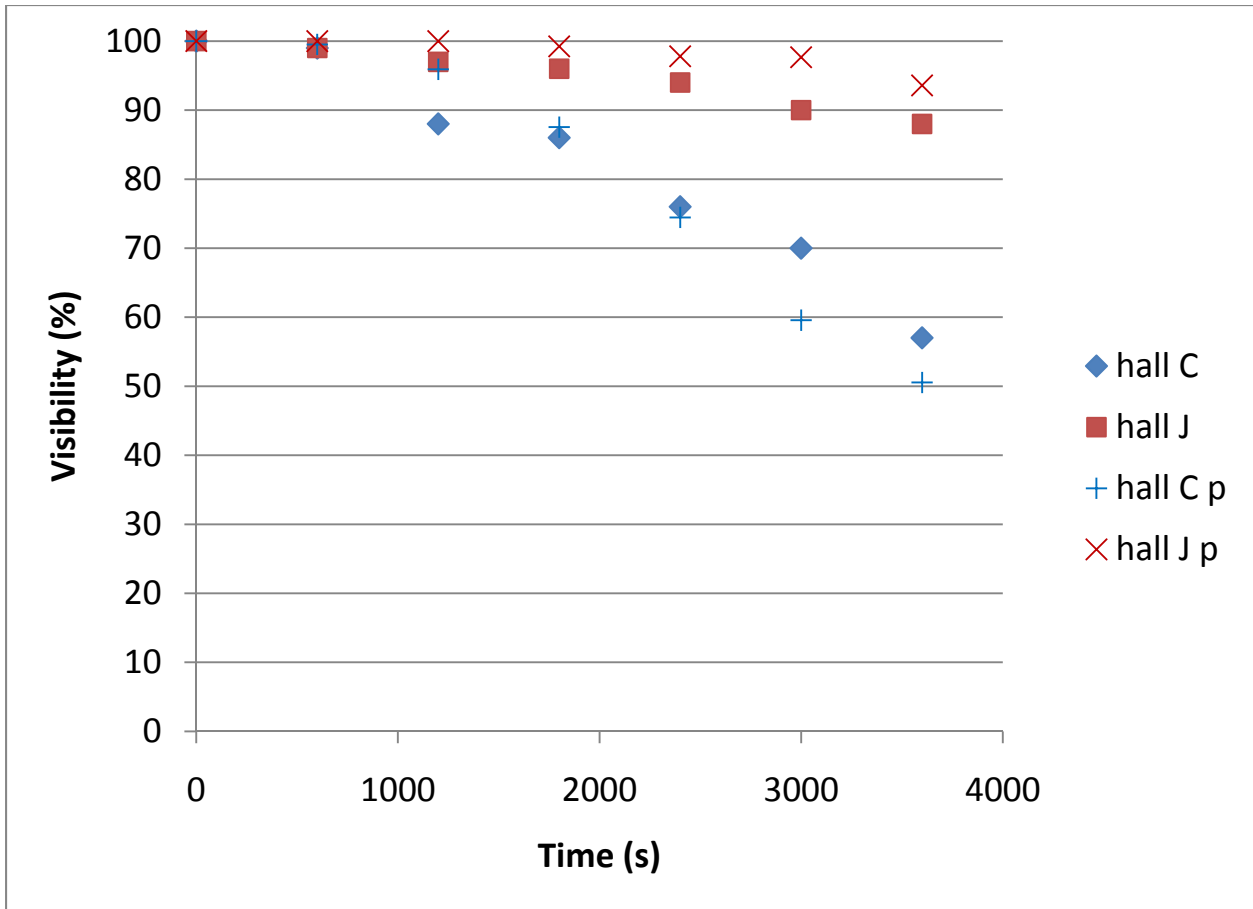


Figure 13 JR-17, Hallway comparisons, NRC peak model. “p” denotes predicted results.

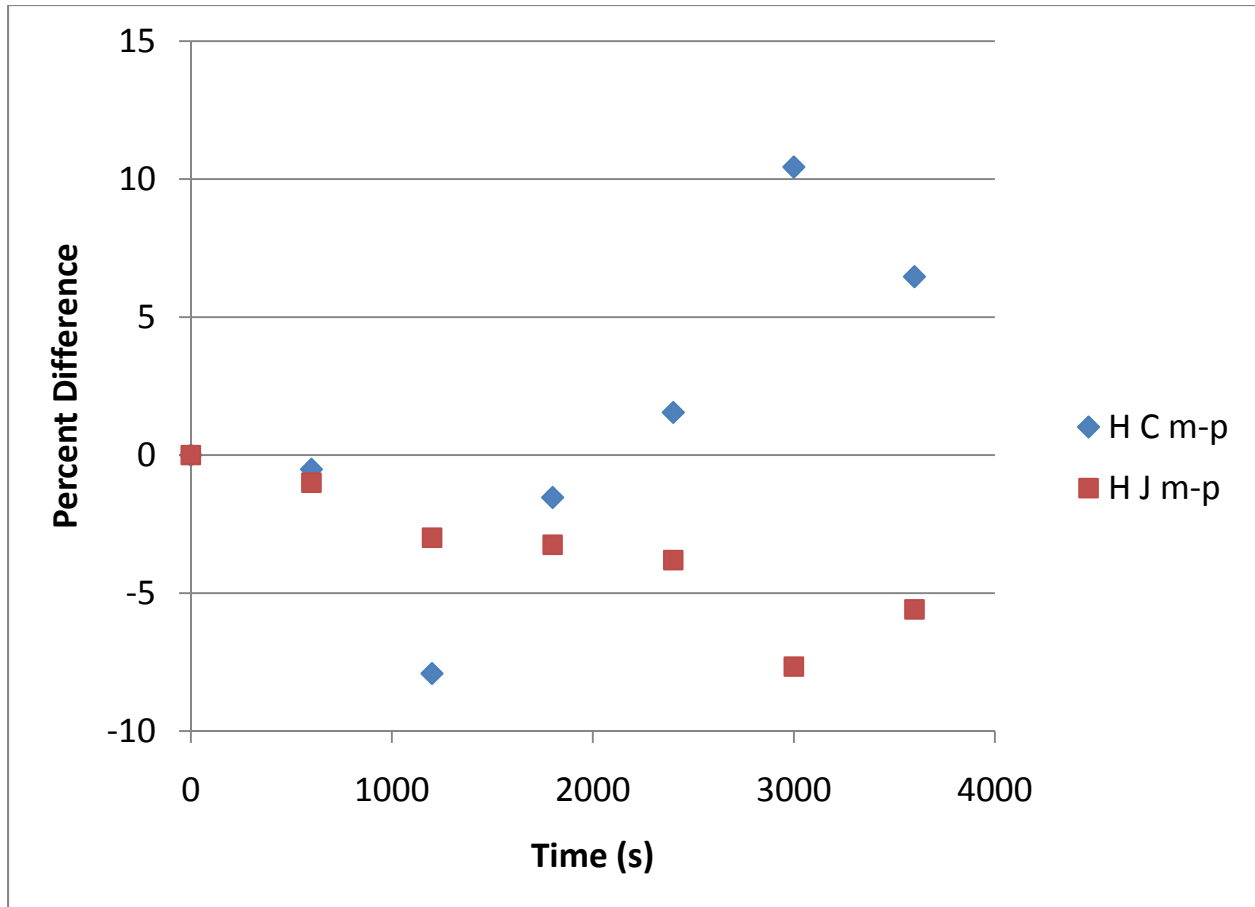


Figure 14 JR-17 Difference between measured (m) and predicted (p) percent visibility for hallways C and J, NRC Peak Model. H stands for hallways.

Experiment JR-19

This smoldering experiment was conducted with the furnace running and all the bedroom doors closed. The flow of smoke through the house should result from the air flow produced by the furnace and movement of smoke through the undercuts of the bedroom doors. The outside temperature was above freezing {0.6 °C to 1.7°C (33 °F to 35 °F)} during the experiment. The temperature changes in rooms throughout the house were recorded only as an initial temperature and a final temperature and these are listed in Table 6. The exception was bedroom A where the temperature was measured throughout the experiment and is given in Table 6.

Room	Bed A	Bed B	Hallway C	Bed E	Bed F	Hallway J
Initial (°C)	21.1	21.7	16.1	15	15	17.8
(°F)	70	71	61	59	59	64
Final (°C)	52.8	20.6	24.4	14.7	14.4	18.6
(°F)	127	69	76	58.5	58	65.5

Table 6 Initial and final temperatures for JR-19

Time (min)	0	15	25	35	45	50	55	60	70	80	90	100	120
Temperature (°C)	21	22	23	24	24	27	28	32	37	40.5	47.8	50.6	50.6
(°F)	70	72	74	75	76	80	83	90	98	105	118	123	123

Table 7 Bedroom A temperatures for JR-19

The temperatures used for modeling included the time-dependent increases measured for bedroom A and a straight line fit connecting initial and final measured temperatures over a 90 minute period for bedroom B and hallways C and J. Rooms that did not have a temperature recorded were assumed to have the same initial temperature as an adjacent room and that temperature was treated as a constant during the calculation.

A thermocouple was attached to a register in the living room to provide a measurement of the temperature flow to that room from the furnace. The temperature at the register varied between 27.8 °C (82 °F) and 53.9 °C (129 °F) with the heating cycle turning on four times during the experiment.

The furnace was operated on automatic and so the furnace blower should turn on at the start of the heating cycle and turn off near the end of the heating cycle. If the temperature rise measured by the thermocouple at the inlet is used to determine the times for blower operation, the blower operated in the periods 0 s to 300 s, 1,200 s to 2,000 s, 2,800 s to 3,500 s and 4,100 s to 4,900 s. Using this measurement for blower operation, the blower operated for approximately 48 % of the time for the 5,400 s experiment. It was assumed for modeling that the flow rates given for the outlets and returns were constant during these time periods and zero otherwise.

Modeling JR – 19 using CONTAM

The smoldering fire was modeled as a smoke source using the Constant Source model and the NRC Peak model. A value of 9,000 µg/s was used for the smoke input for the Constant Source model. The constants used for the NRC Peak model included a smoke input of 12,000 µg/s, 0.85 for the filtering constant, and 1.5 hr. for the peak time. These constants were chosen in order to approximate the measured visibility in bedroom A where the mattress smoldered.

The constant source model underestimated the visibility in bedroom A, Figure 15 and Figure 16, for the first 2,500 s of the experiment and then provided nearly identical results for the next 2,500 s. The predicted visibility for bedrooms B and F were almost identical and more closely agreed with the visibility measurements in bedroom B.

The NRC peak model provided qualitative visibility predictions for bedroom A, Figure 17 and Figure 18, throughout the experiment. The predicted visibility for bedrooms B and F were nearly identical with the predictions closer in agreement with the visibility measurements in bedroom B.

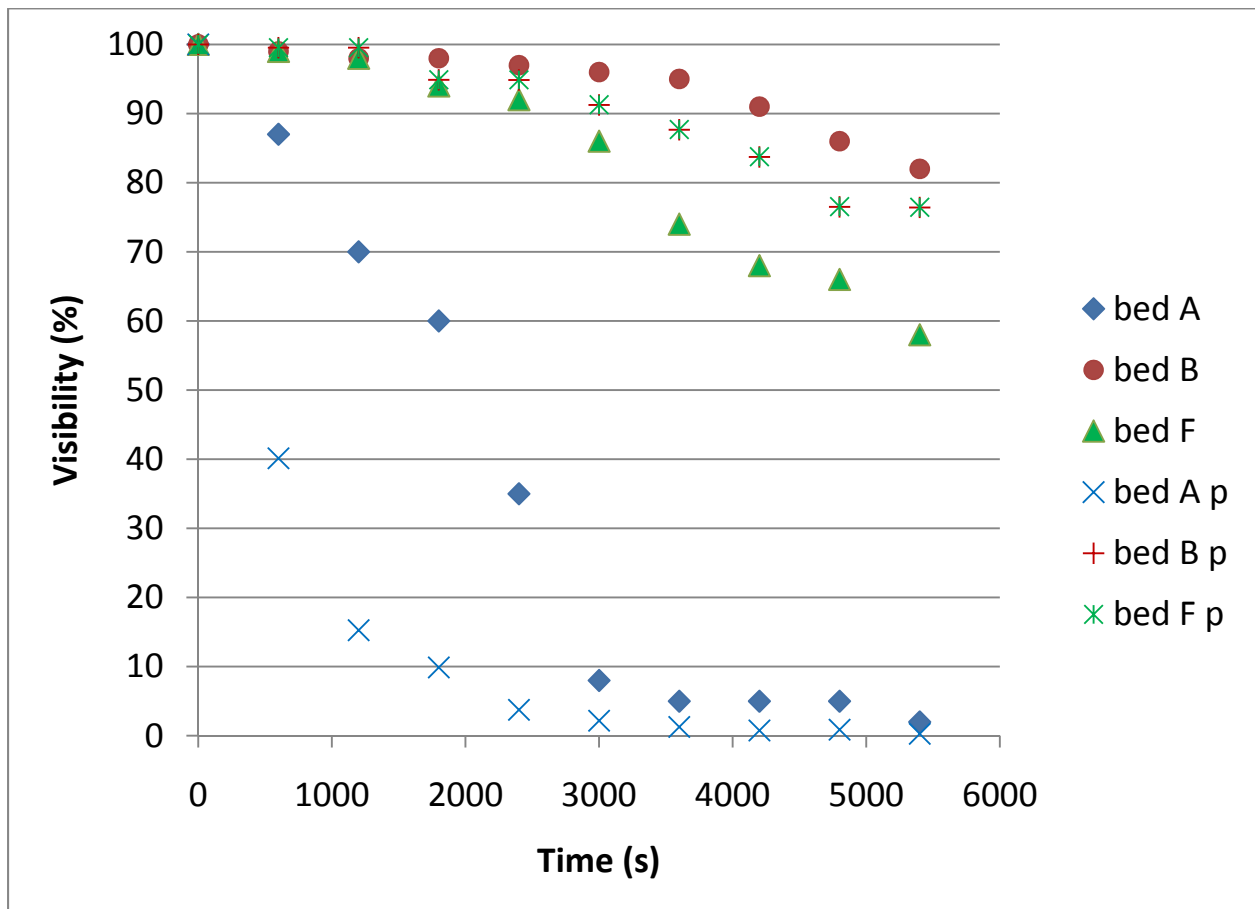


Figure 15 JR -19 Bedroom comparisons, Constant Source model. "p" denotes predicted results.

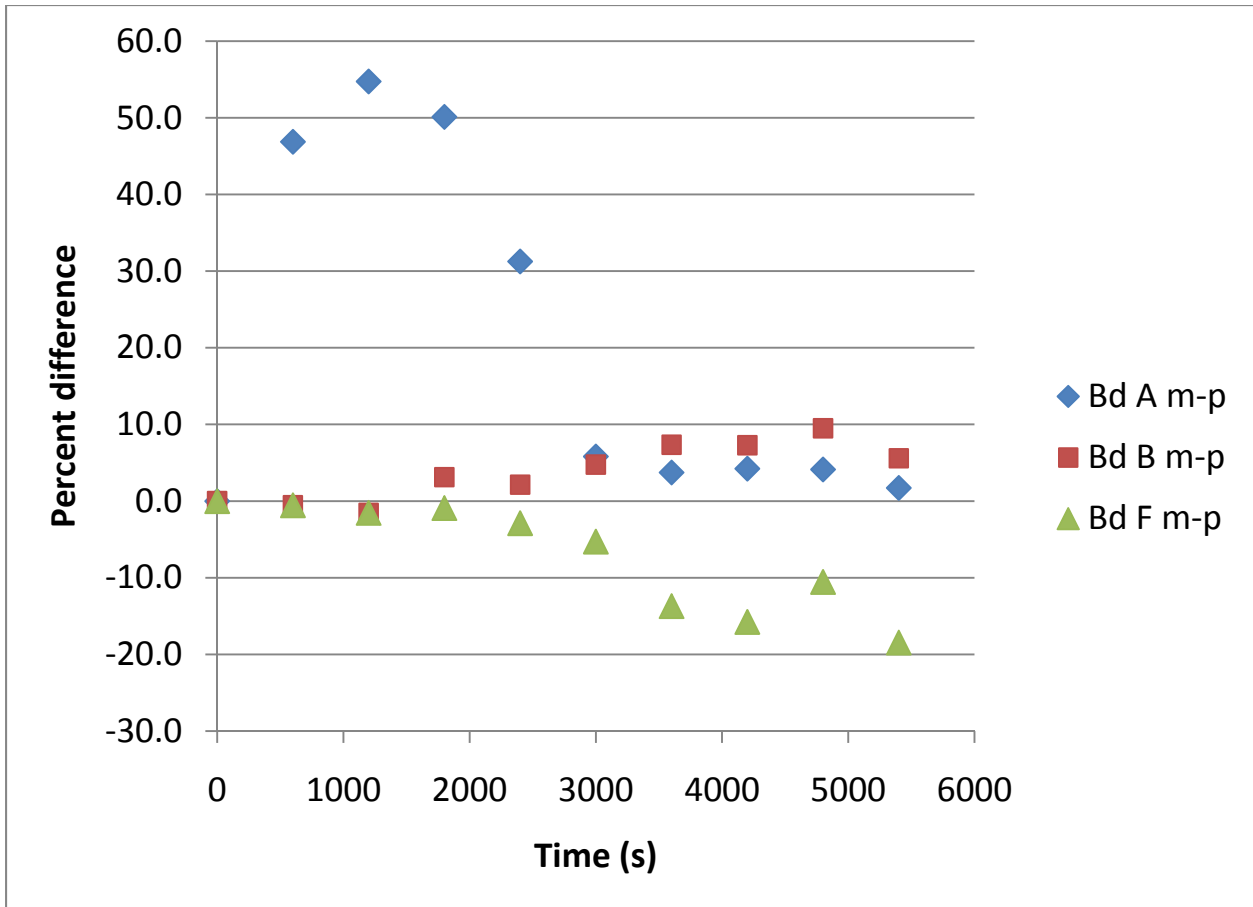


Figure 16 JR-19 Difference between measured (m) and predicted (p) percent visibility for bedrooms A, B, and F, Constant Source. Bd stands for bedroom.

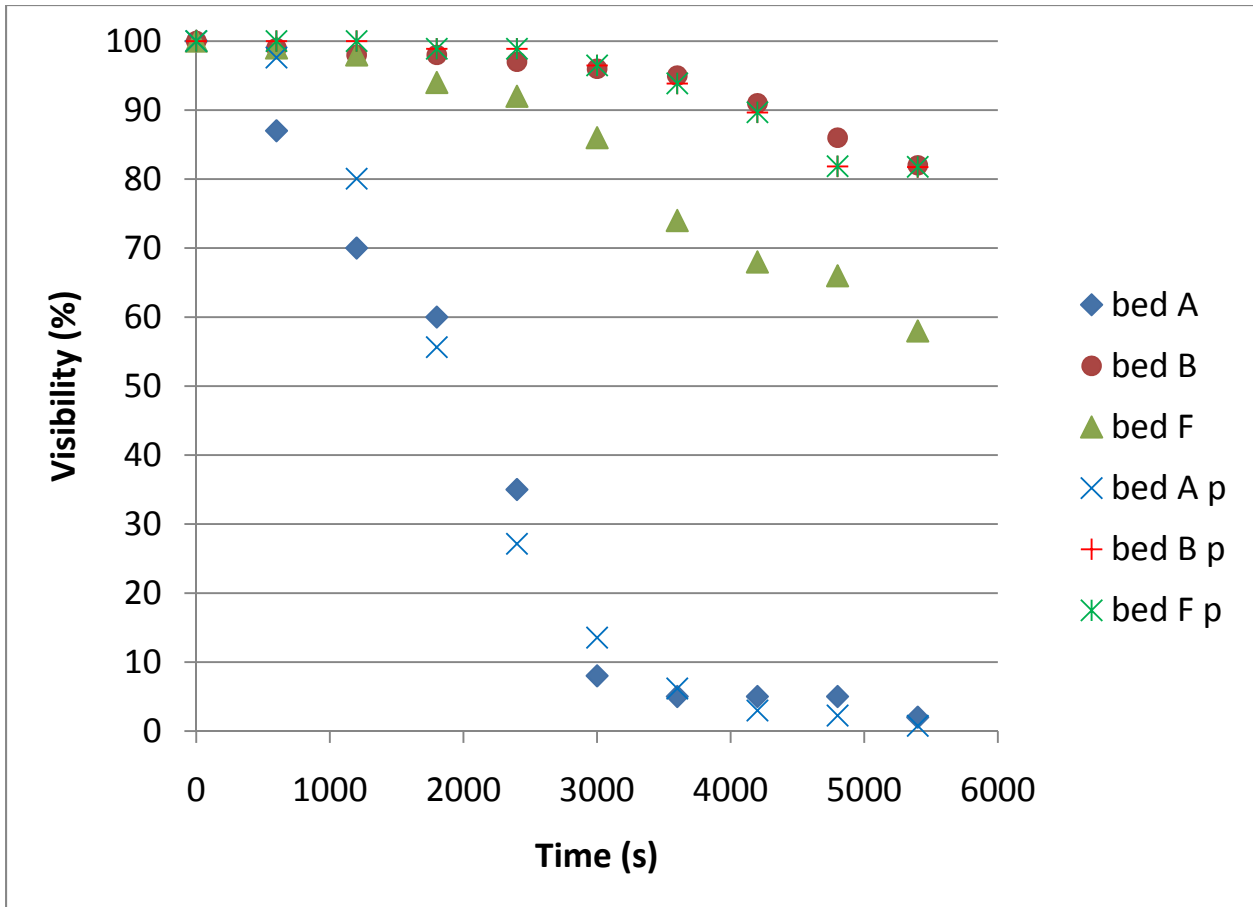


Figure 17 JR-19 bedroom comparisons, NRC peak model. "p" denotes predicted results.

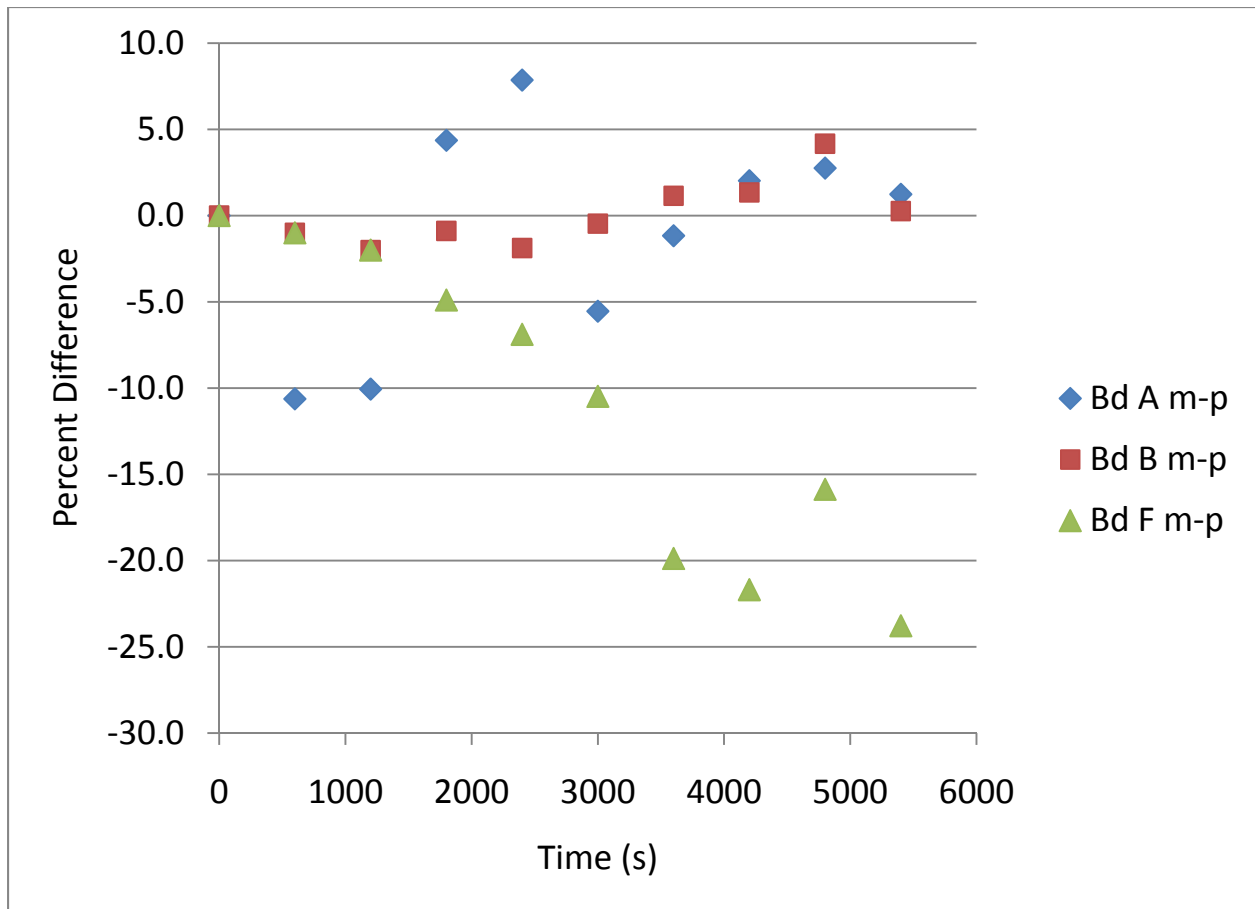


Figure 18 JR-19 Difference between measured (m) and predicted (p) percent visibility for bedrooms A, B, and F, NRC Peak Model. Bd stands for bedroom.

Both models predicted more visibility in the hallways than was measured, Figure 19 and Figure 21. Using Figure 20 and Figure 22, the upstairs hallway J was better represented than the downstairs hallway C with the constant source model predicting the visibility of hallway J more accurately while the NRC Peak model predicted the visibility more accurately for hallway C. An issue that might explain at least some of the underestimate in visibility is the use of the measured hallway temperatures in the modeling. The relatively large increase in the temperature of hallway C was assumed to occur over a 90 minute period. This temperature increase should drive smoke from the downstairs hallway to other rooms on the first floor thereby reducing the amount of smoke in this hallway and also reducing the amount of smoke flowing up the stairs to the upstairs hallway.

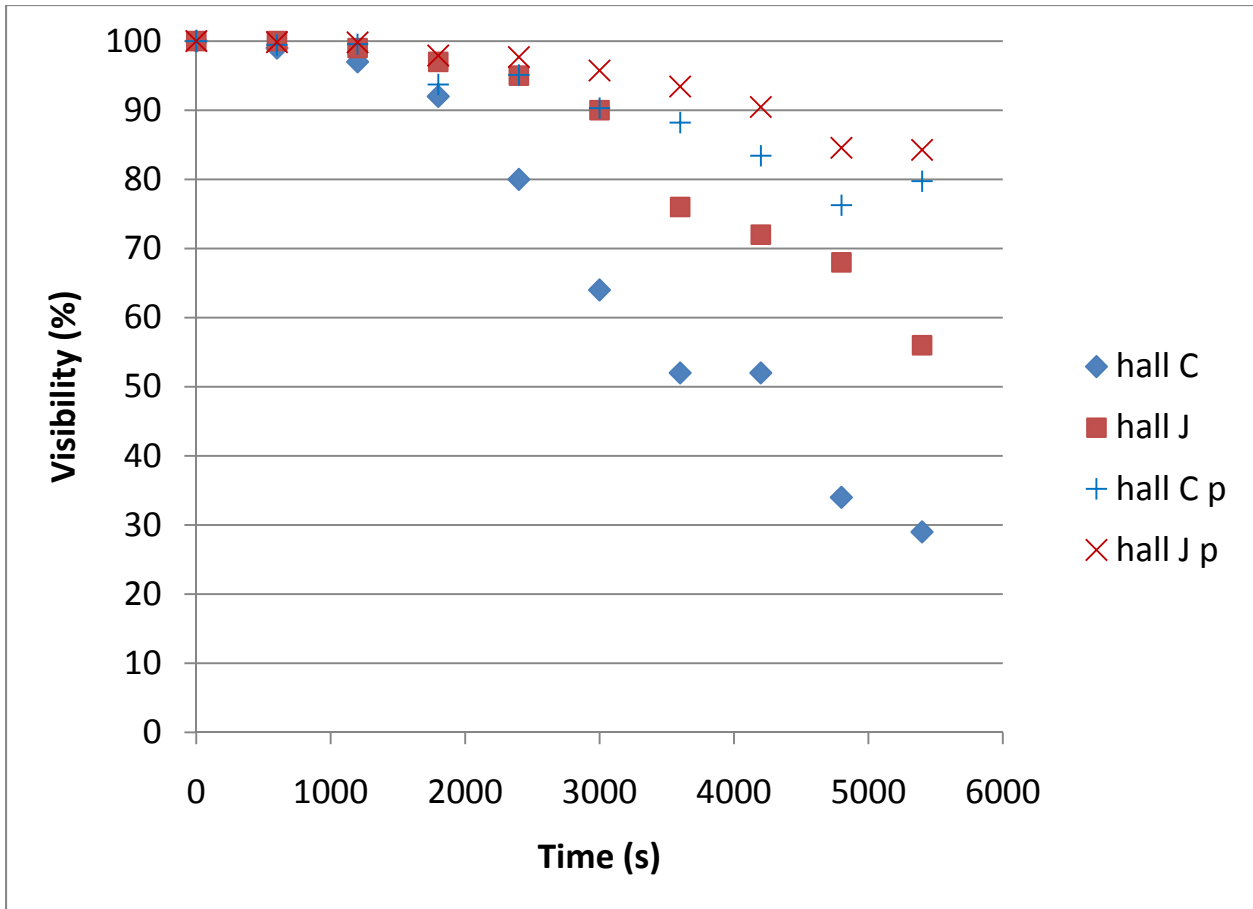


Figure 19 JR-19 hallway comparison, Constant Source. "p" denotes predicted results.

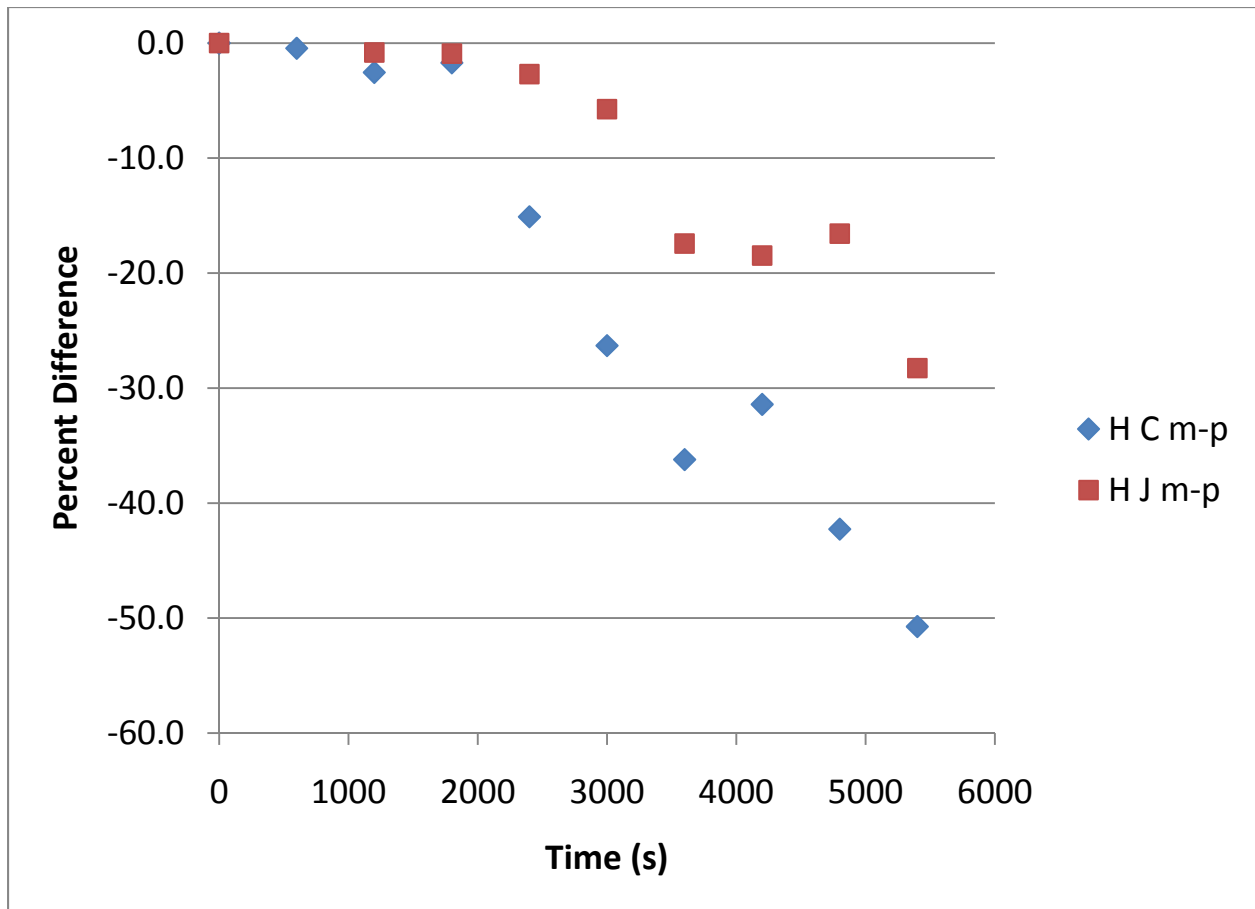


Figure 20 JR-19 Difference between measured (m) and predicted (p) predicted visibility for hallways C and J, Constant Source. H stands for hallways.

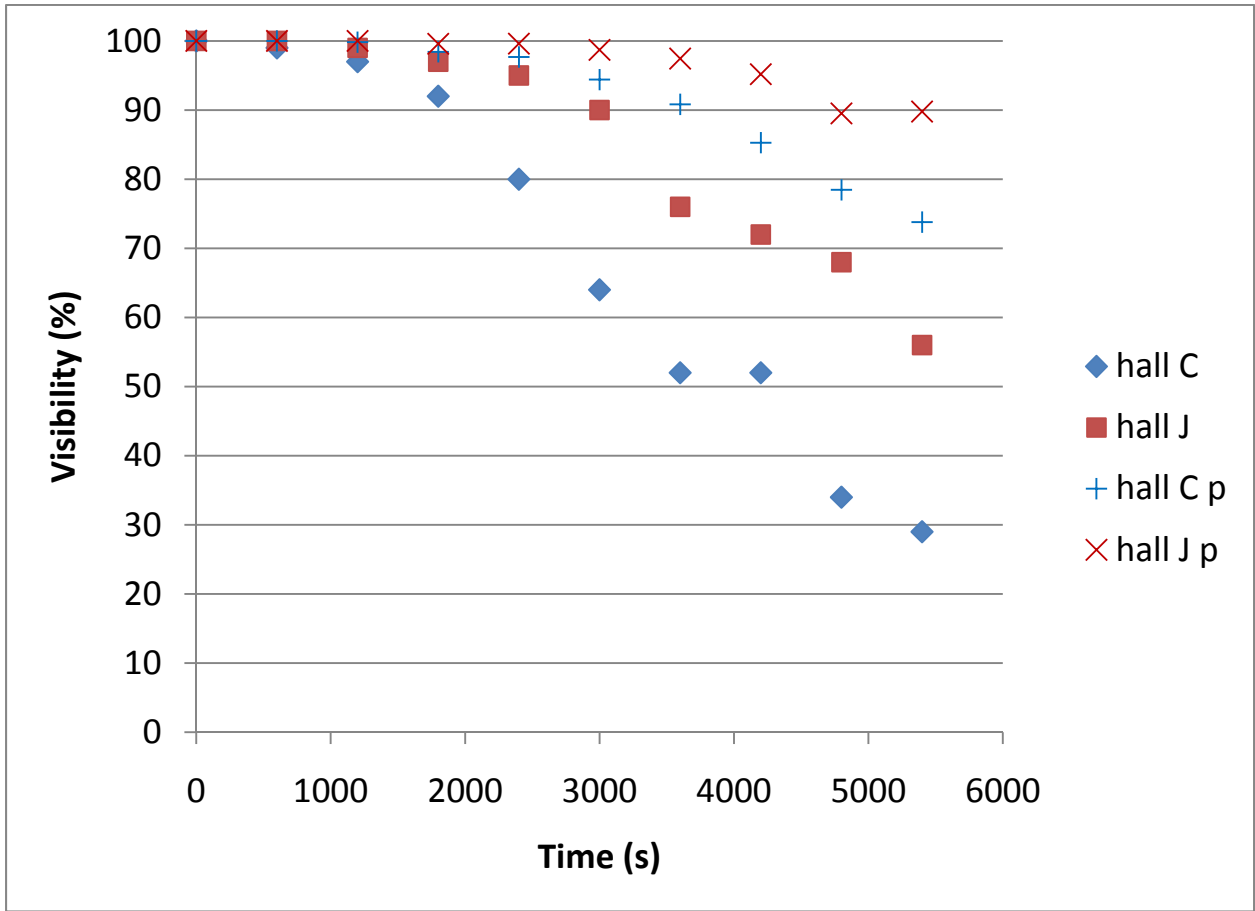


Figure 21 JR-19 hallway comparison, NRC peak model. "p" denotes predicted results.

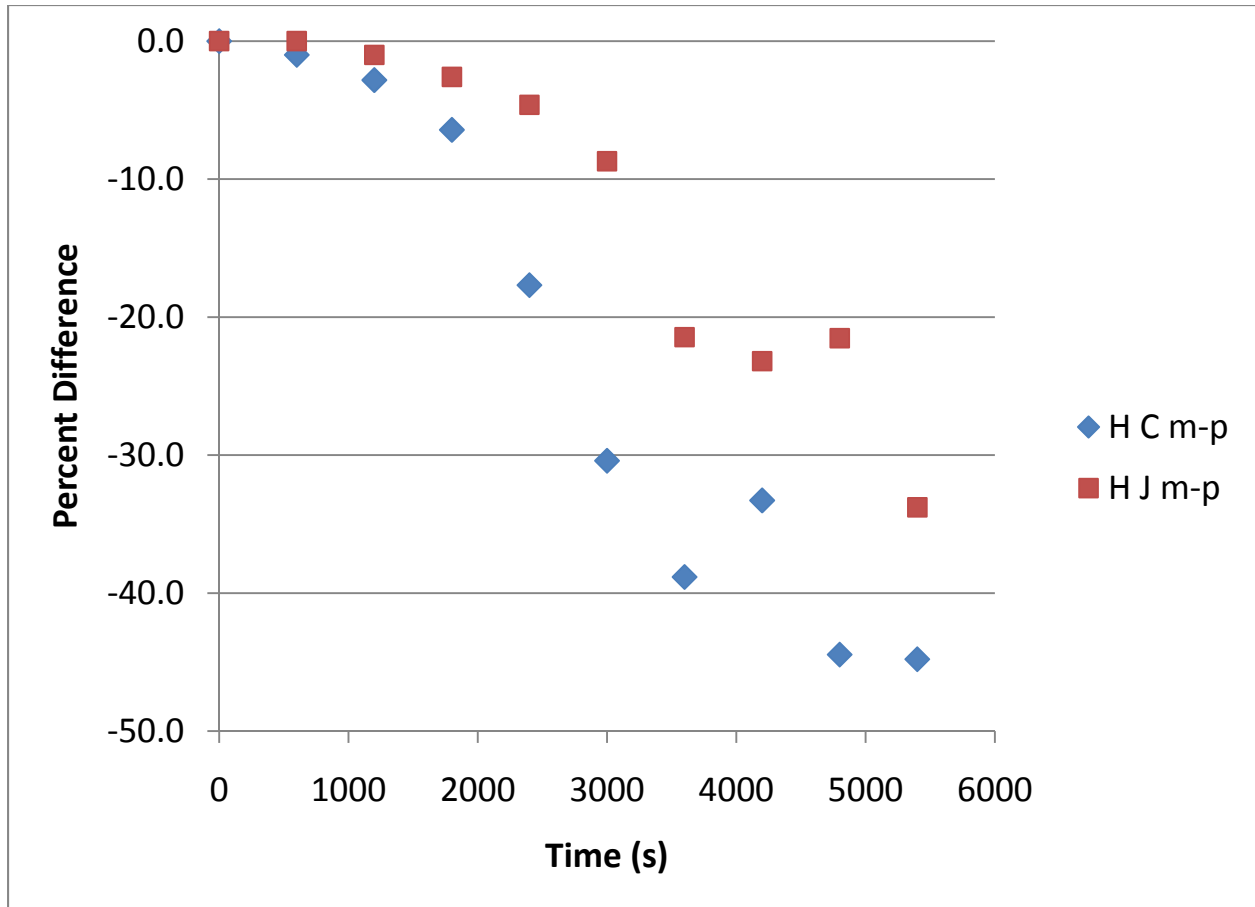


Figure 22 JR-19 Difference between measured (m) and predicted (p) percent visibility for hallways C and J, NRC Peak Model. H stands for hallways.

Optical Density Comparison

A comparison of the measured optical densities at the ceiling in bedroom A for the three experiments, Figure 13, shows that at times earlier than 1,200 s, the optical densities from the three experiments are reasonably consistent but after 1,200 s, the optical density for experiments JR-18 and JR-19 increase rapidly compared to JR-17. At 2,100 s, the optical density for JR-19 starts to increase more than the optical density for JR-18 and starting at 2,700 s, JR-19 optical density becomes much greater than JR-18. The differences in the experiments that may account for the smoke buildup is that bedroom A door was closed for JR-19 but was open for the other experiments. The furnace was not operating for JR-18 but operated for the other two experiments. Since JR-19 had the largest optical densities that would imply that smoke

movement through the door is more important than the smoke movement produced by the furnace assuming that the amount of smoldering was consistent for all experiments.

Observation of the extent of charring is only approximate. For JR-17, the charred area was 0.41 m (16 in) in diameter at 3,600 s with the char having gone through the bottom of the mattress; for JR-18 the charred area was 0.46 m (18 in) in diameter with a 0.25 m (10 in) diameter center that was burned out at 3,600 s; for JR-19 the charred area was 0.41 m (16 in) in diameter at 2,700 s. There was no report of how far the mattress had burned through and no report at 3,600 s. Based on these observations, the charring observed for the three burns appeared to be similar.

The measured temperature at the ceiling in bedroom A is another indicator of how important the open door/closed door is for experiments JR-17 and JR-19. The temperature for JR-17 remained fairly constant over the 3,600 s time period while the temperature measured for JR-19 gradually increased. This increase in temperature suggests that the closed door prevented the heat from smoldering to escape. The increasing temperature after 3,000 s may have enhanced the rate of smoldering which would explain the increased optical density observed for JR-19.

Comparing JR-18 with JR-17, the difference is that the furnace was operating for JR-17 but not JR-18 and the doors to the other bedrooms were closed for JR-18. The higher observed optical density for JR-18 may partially be the result of the furnace moving smoke from bedroom A to other rooms in the house for JR-17 and partially the result of the doors to the three bedrooms being closed for JR-18 reducing the house volume and eliminating some air leakage.

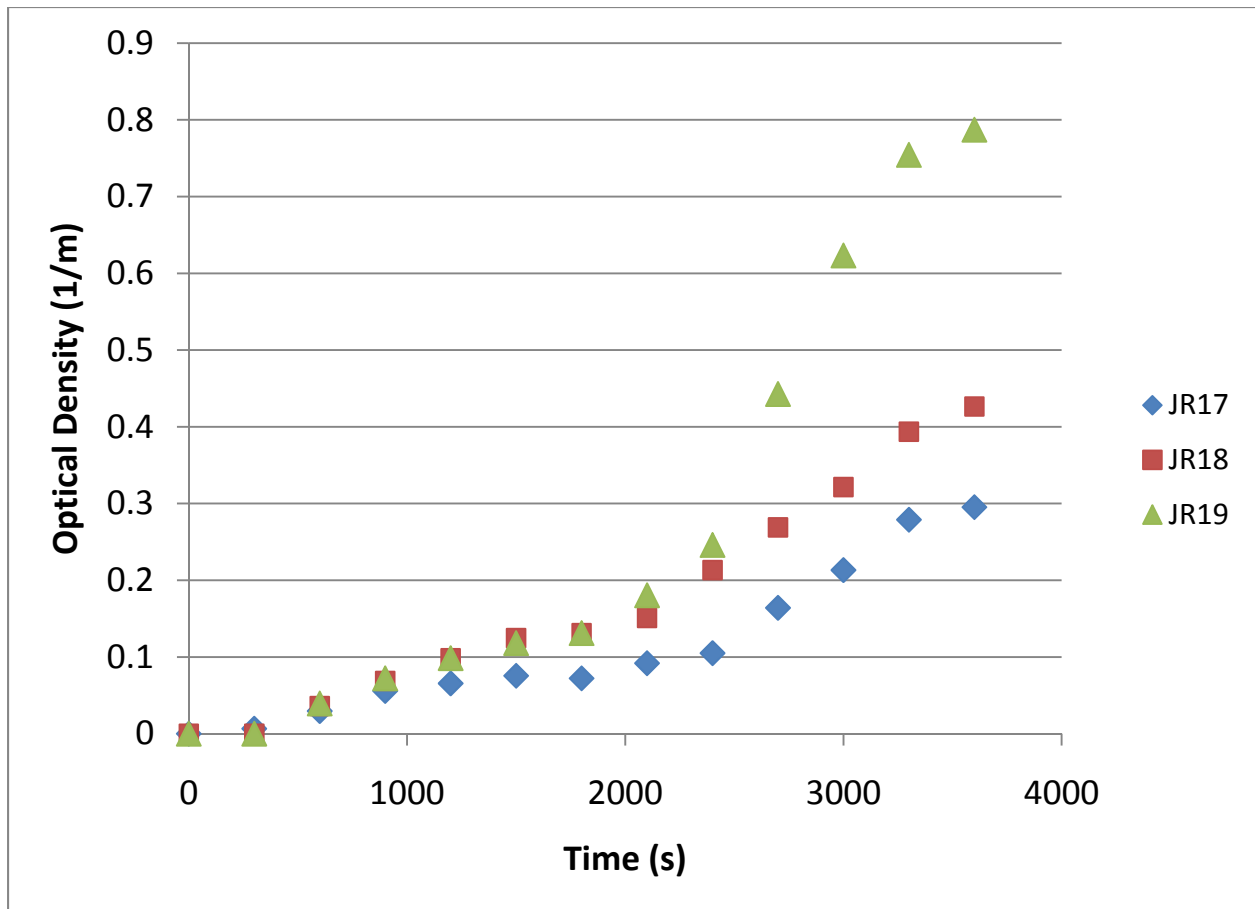


Figure 23 Comparison of the measured optical density at the ceiling for the three experiments. Measurement points are shown at 300 s intervals.

Comparing JR-17 with JR-19 also supports the idea that smoke movement out the door of bedroom A dominated the smoke extraction by the furnace system as the optical density in bedroom A for JR-19 is significantly higher than JR-17 as the furnace is operating for both tests but the bedroom A door is closed for JR-19.

Examining the optical density measured at 1.5 m (5 ft) above the floor in bedroom A as shown in Figure 14 supports the observations using the optical density at the ceiling. The biggest difference between the two measurement heights is that JR-17 and JR-18 optical densities at 1.5 m (5 ft) are closer in value but JR-18 optical densities are still larger. JR-17 optical density increase begins to lag the other two experiments at 1200 s for both the ceiling and 1.5 m (5 ft) measurements. JR-19 optical density starts to exceed JR-18 optical density at 1,800 s for the 1.5 m (5ft) measurement and at 2,100 s for the measurement at the ceiling.

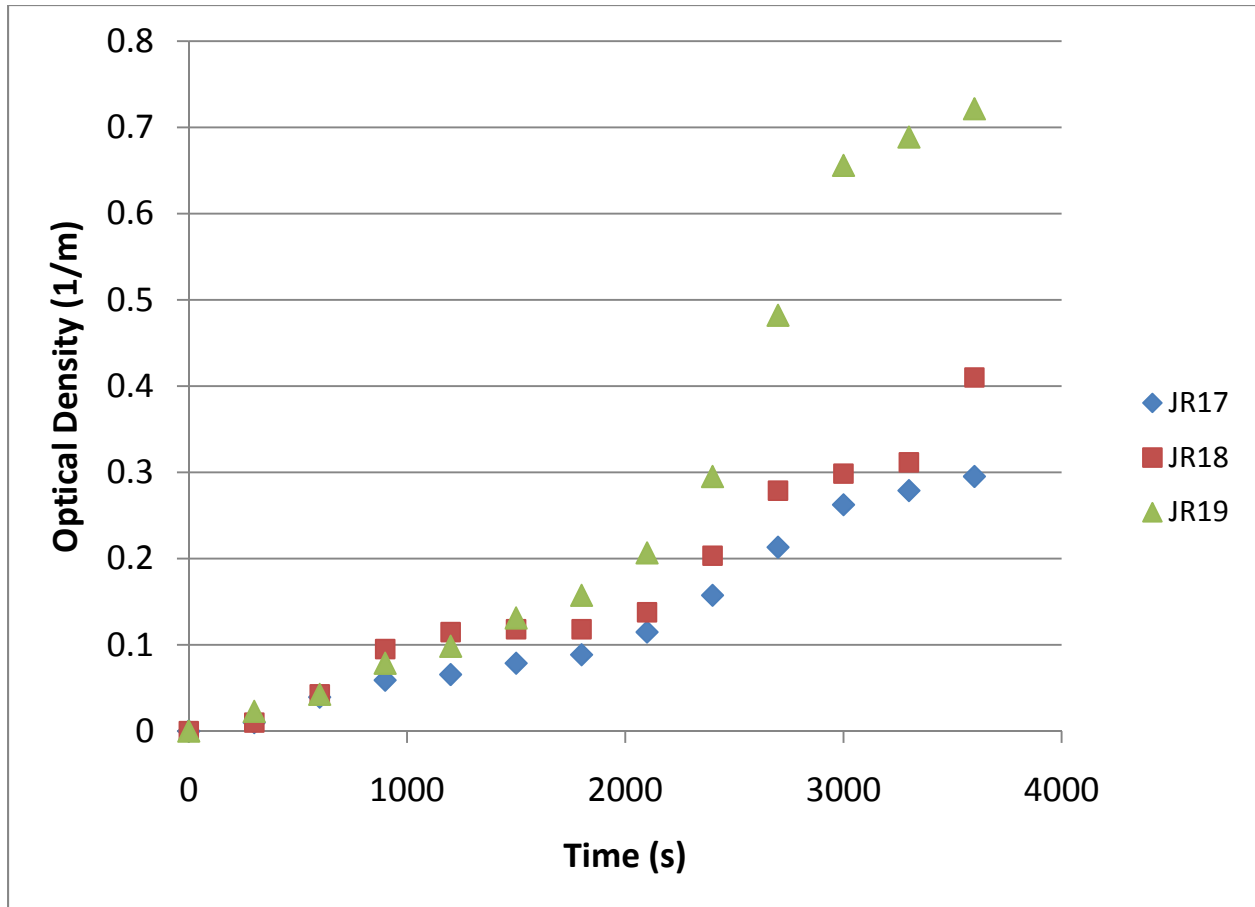


Figure 24 Optical densities for the three experiments measured 1.5 m (5 ft) above the floor. Measurement points are shown at 300 s intervals

Comparing the optical density measurements at 1.5 m (5 ft) above the floor and at the ceiling for bedroom A provides insight in determining how well-mixed the smoke was at these elevations. Figure 25 provides the percent difference between the ceiling measurement and the 1.5 m (5 ft) measurement. The percent difference was calculated using

$$\text{percent difference} = 200 * (OD(c) - OD(1.5)) / (OD(c) + OD(1.5))$$

where OD(c) was the optical density at the ceiling and OD(1.5) is the optical density at 1.5 m (5 ft) above the floor. The optical density percent differences for JR-18 and JR-19 are small and suggest that the smoke is well-mixed. The percent differences for JR-17 may indicate a higher smoke concentration at 1.5 m (5 ft) than at the ceiling but there are sufficient measurements near zero percent difference to suggest that the smoke was well mixed during this experiment.

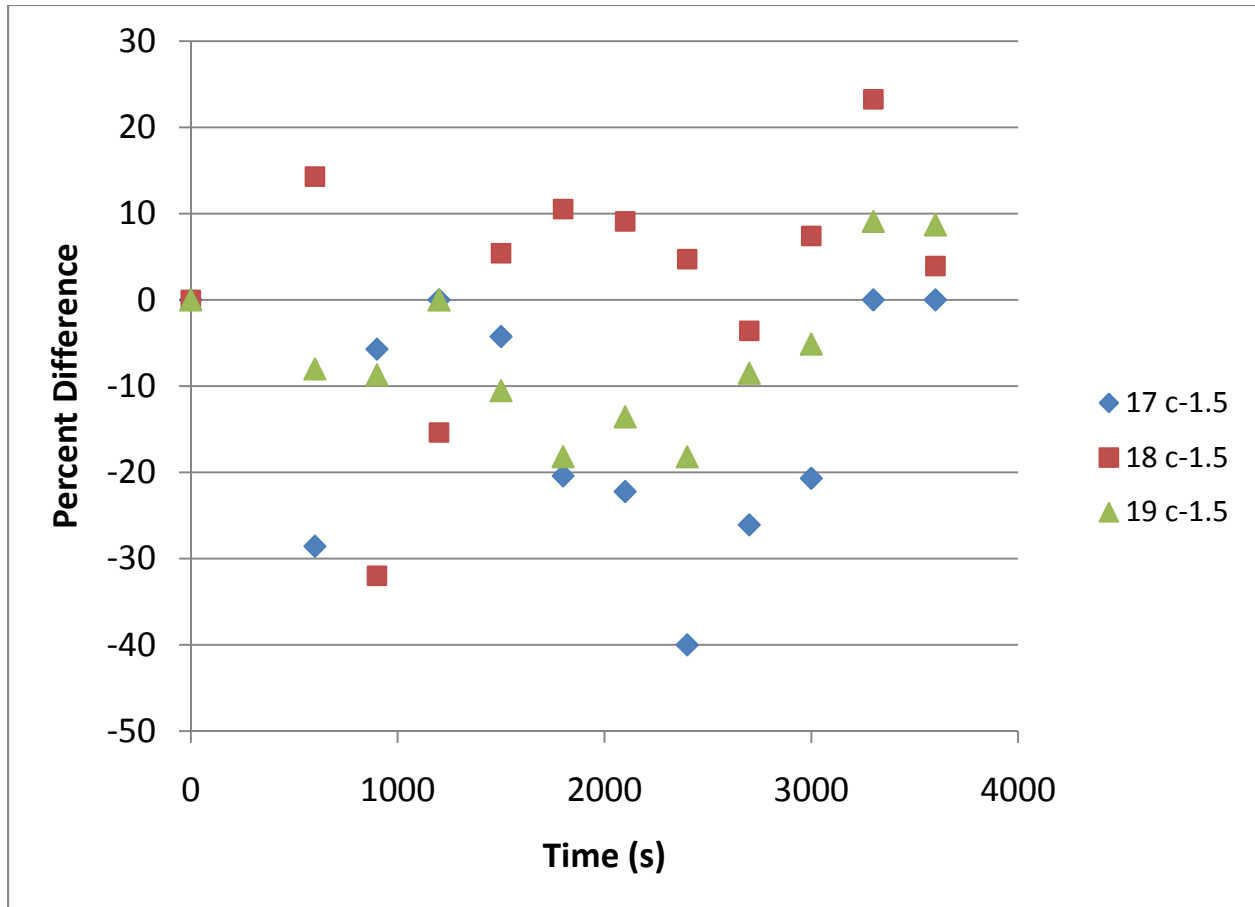


Figure 25 Percent difference between the optical density at the ceiling (c) and at a height of 1.5 m (5 ft) above the floor (1.5) for the three experiments

Uncertainty

The experiments modeled² using CONTAM⁴ were reported with no uncertainty analysis. The measurements used to extract the information for the modeling included measurements of room size, white light attenuation for visibility, temperature using thermocouples, and average volume flow for inlet registers and returns. The length measurements should be quite accurate with uncertainties on the order of 5 % or less and the accuracy of the temperature measurements should be on the order of 1.0 °C. The white light attenuation measurement should show a one sigma random noise component of ±20 %. The one sigma uncertainty in the volume flow measurements could be approximately ±20 % but there is no way to validate this estimate.

The systematic errors could have a larger impact on the results than the uncertainties discussed in the preceding paragraph. These errors or omissions include:

- Temperatures not measured for all spaces,

- Temperature information for a space only provided at two times,
- Obscuration measurements made for only some spaces and restricted to two elevations, at the ceiling and 1.5 m (5 ft) above the floor,
- Long-term stability of the light source used for the obscuration measurements
- Impact of the weather not measured inside the house,
- Door geometry for the undercuts not provided.

Each of these omissions had an impact on the modeling results with the lack of temperature measurements particularly impacting the modeling comparisons for experiment JR-19 as discussed in the experiment section and the conclusion.

Conclusion

Even for the low temperatures produced in these smoldering experiments it was obvious that smoke flow through the fire room door dominated the extraction and spread of smoke by the furnace. A summary of the application of CONTAM to predict the visibility in hallways and bedrooms using the visibility measured in the fire room as a measure of the smoldering is shown in table 8 where the maximum visibility difference for each bedroom and hallway is given. A measure of the modeling accuracy is to look at the instances where the modeled visibility differed by more than 25 % from the measured visibility. Using the NRC Peak model, only three out of fifteen spaces had a predicted visibility that was greater than 25% of the measured visibility while the Constant Source model had nine such differences. The lack of time-dependent temperature data for many of the rooms in the house impacted the modeling as the smoke flow to these areas could not be accurately calculated.

Space	JR - 17		JR - 18		JR - 19	
	Visibility Difference (%)	Difference Greater than 25 %	Visibility Difference (%)	Difference Greater than 25 %	Visibility Difference (%)	Difference Greater than 25 %
Constant Source Model						
Bedroom A	40	X	30	X	60	X
Bedroom B	50	X			10	
Bedroom F	10				20	
Hallway C	30	X	40	X	30	X
Hallway J	5		40	X	60	X
NRC Peak Model						
	Visibility Difference (%)	Difference Greater than 25 %	Visibility Difference (%)	Difference Greater than 25 %	Visibility Difference (%)	Difference Greater than 25 %
Bedroom A	10		20		10	
Bedroom B	30	X			5	
Bedroom F	20				25	
Hallway C	15		25		50	X
Hallway J	10		25		40	X

Table 8 Summary of the modeling results tabulating the largest difference in the predicted and measured visibility.

The impact of the wind on the smoke spread was not included in the modeling. The only weather impact that was included was the cooling of the second floor with the furnace off which caused the smoke to be drawn up the stairs to the second floor hallway. CONTAM did predict that the second floor hall visibility would be less than the visibility in the first floor hallway with some accuracy which would suggest that wind effects were not important for the hallway visibilities.

CONTAM was not designed to be a predictive model for smoke flow from smoldering fires. To become a predictive model, an algorithm to provide HRR, smoke and CO production needs to be included in CONTAM. A second algorithm to provide a mechanism to heat rooms based on the smoldering fire's HRR would then complete the necessary model development.

This set of experiments provides data to explore modeling of smoke movement in the presence of smoldering fires. Additional experimentation is desirable to understand smoke movement in the presence of modern HVAC systems using tests where the HRR and smoke fraction of the smoldering material are measured and temperature measurements are available for all spaces in the test facility. At a minimum, additional experiments should provide the necessary comparisons to develop a smoldering input model for CONTAM and provide additional insight into the importance of including HVAC systems in models used for understanding smoke movement in residential spaces.

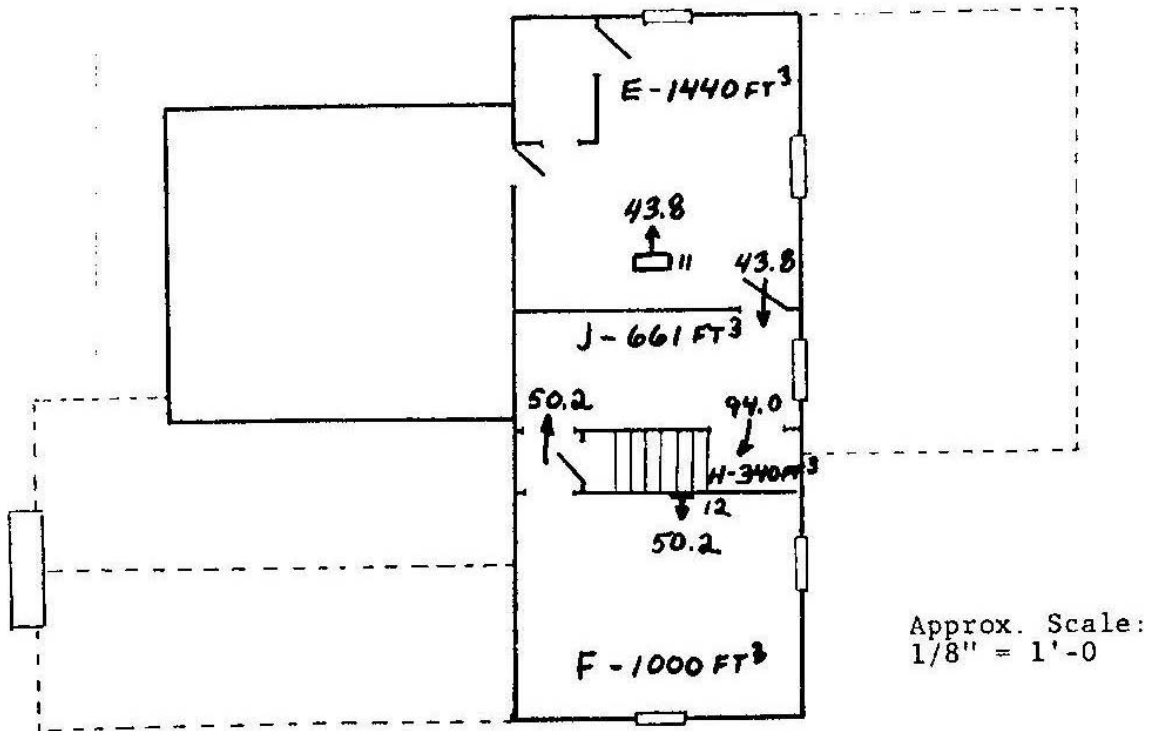


Figure 27 second floor with all bedroom doors open.

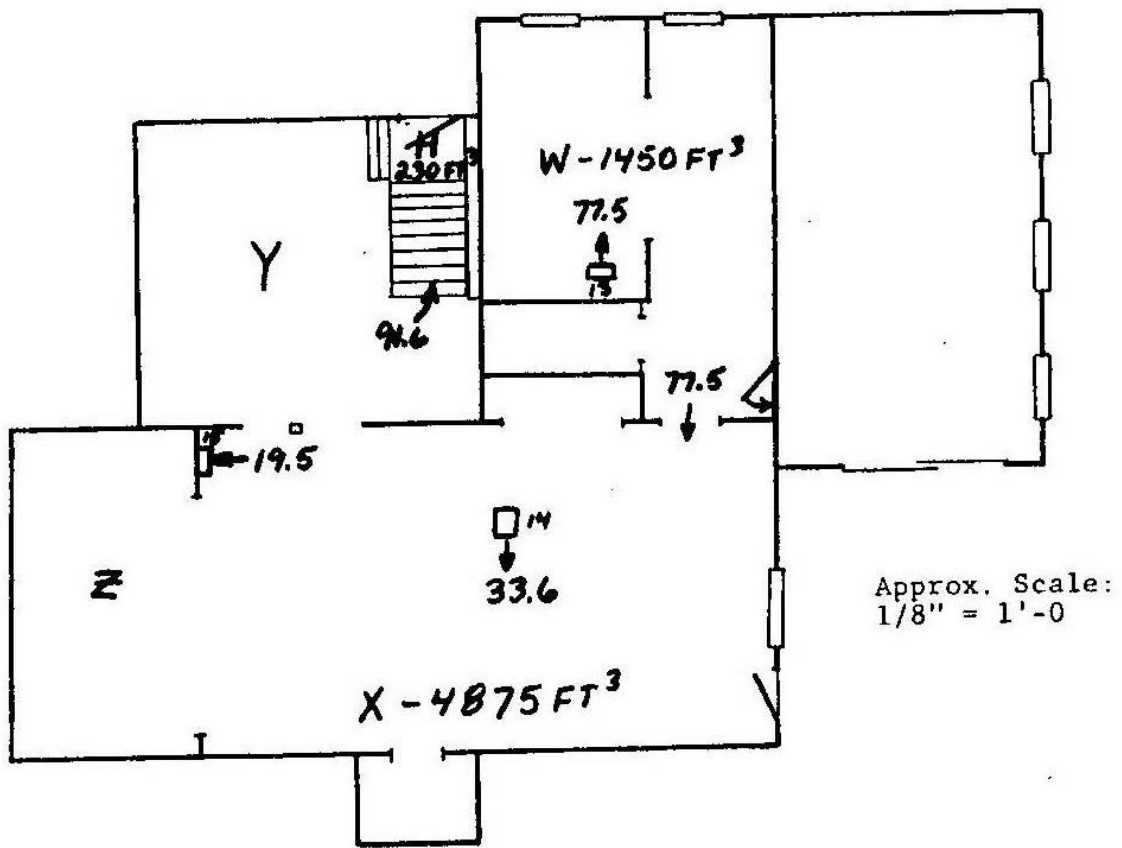


Figure 28 basement with all bedroom doors open. The furnace is located in space Z.

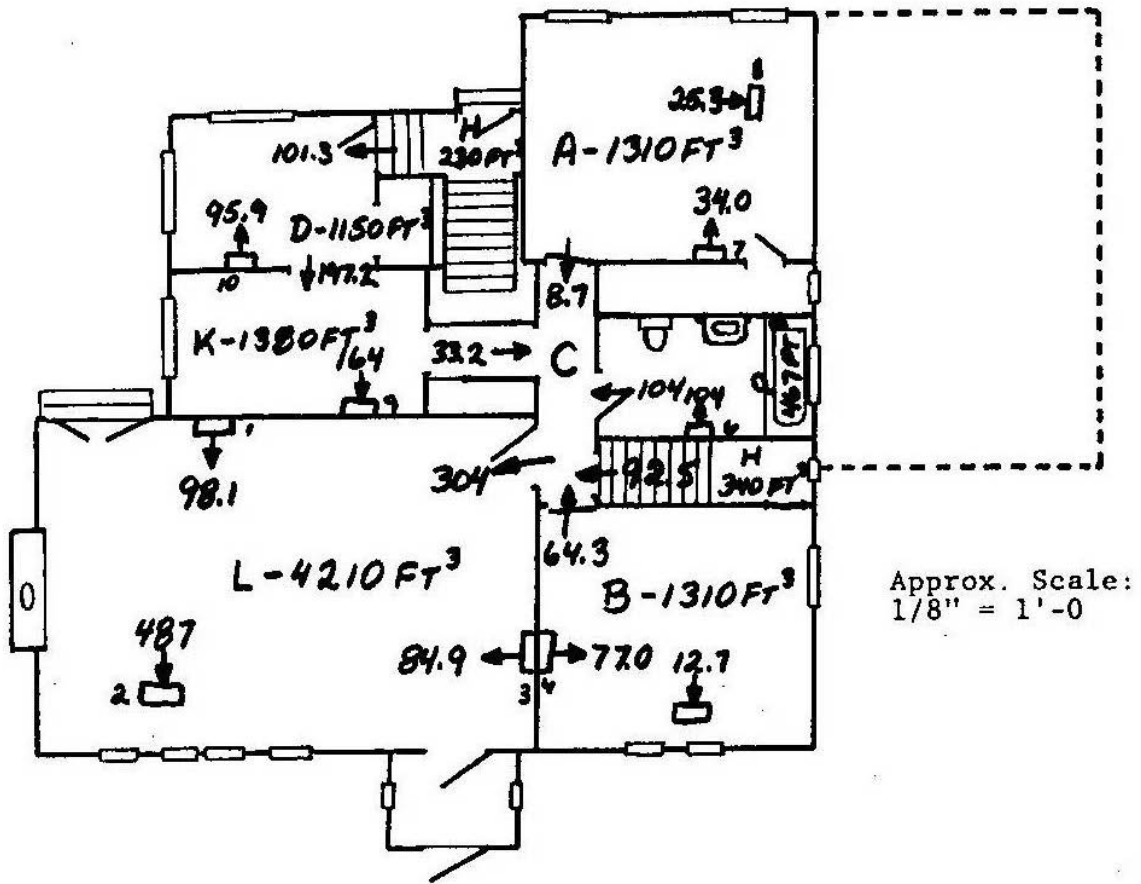


Figure 29 first floor with all bedroom doors closed.

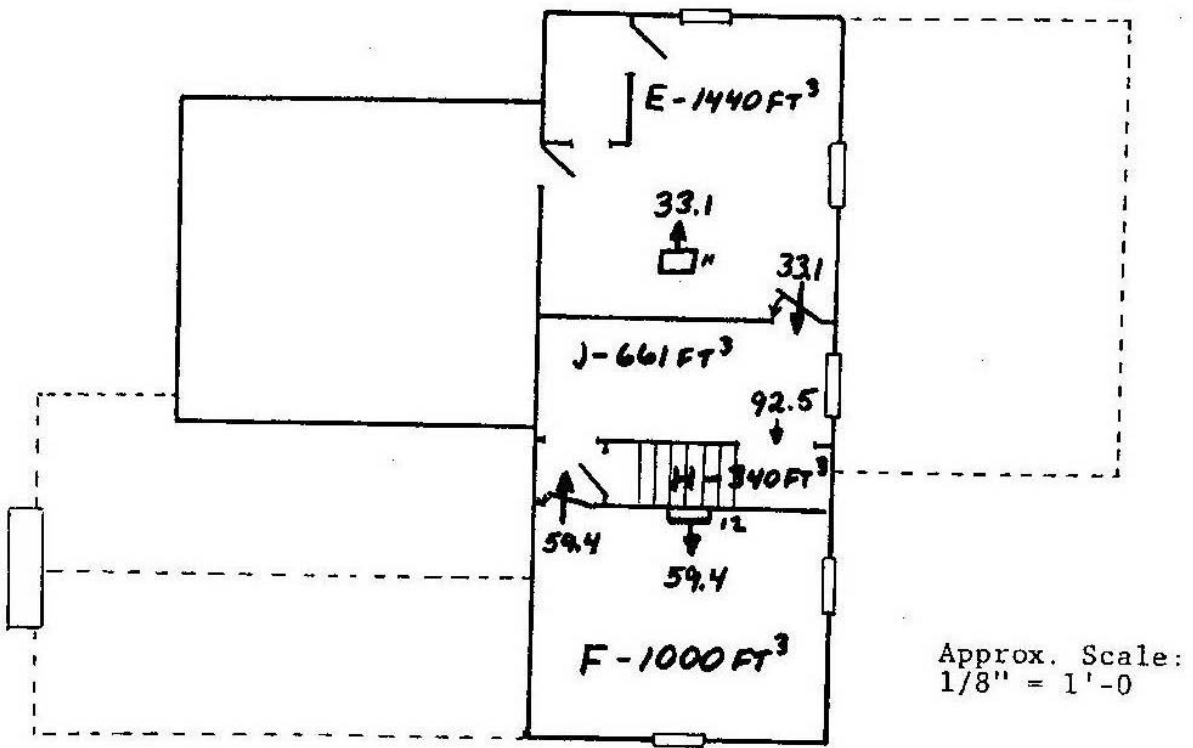


Figure 30 second floor with all bedroom doors closed.

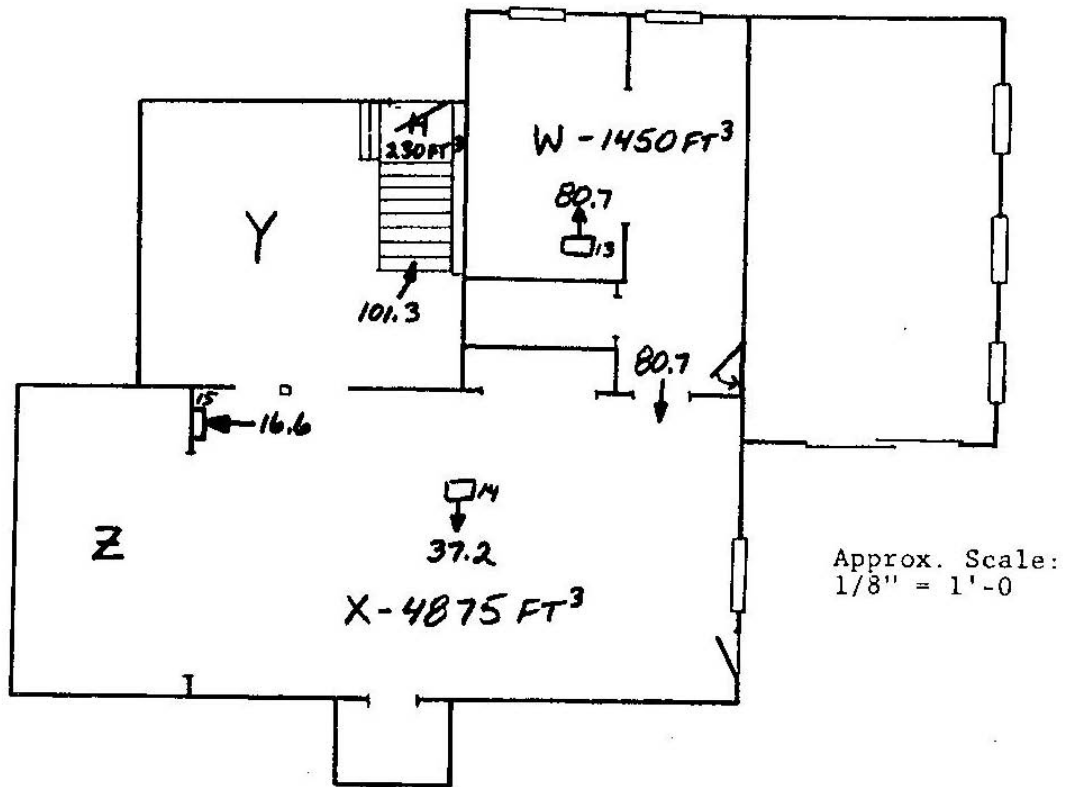


Figure 31 basement with all bedroom doors closed. The furnace is located in space Z.

References

- ¹ Ohlemiller, T. J., "Smoldering Combustion", The SFPE Handbook of Fire Protection Engineering 3rd ed., (2002) 2-200.
- ² Bukowski, R. W., Waterman, T. E., and Christian, W. J., "Detector Sensitivity and Siting Requirements for Dwellings," NBS GCR 75-51, National Institute of Standards and Technology, (1975) pp. 1-171.
- ³ Bukowski, R. W., Rolf Jensen and Associates, Private Communication (2010).
- ⁴ Walton, G.N. and W.S. Dols. "CONTAM 2.1 Supplemental User Guide and Program Documentation," NISTIR 7049, National Institute of Standards and Technology (2003) pp. 1 – 101.
- ⁵ Seader, J. D. and Einhorn, I. N., 16th Symposium (international) on Combustion, Combustion Institute, (1976).
- ⁶ Mulholland, G. W., "Smoke Production and Properties," The SFPE Handbook of Fire Protection Engineering 3rd Edition, (2002), 2-263.